Premeiotic and meiotic failures associate with hybrid male sterility in the *Anopheles gambiae* complex

Short title: The cellular basis of hybrid male sterility in malaria mosquitoes

Jiangtao Liang[1], Igor V. Sharakhov[1,2,*]

[1]Department of Entomology, Virginia Polytechnic Institute and State University, Blacksburg, Virginia, United States of America

[2]Department of Cytology and Genetics, Tomsk State University, Tomsk, Russian Federation

[*]**Corresponding author**

E-mail: igor@vt.edu

Abstract

Hybrid male sterility contributes to speciation by restricting gene flow between related taxa at the beginning stages of postzygotic isolation. However, we have limited knowledge about cellular processes and molecular mechanisms that come into play when fertility is first affected. Hybrids between closely related species of the *Anopheles gambiae* complex offer opportunities to identify spermatogenic errors that arise early during speciation. To investigate possible cellular causes of hybrid male sterility, we performed crosses between sibling species of the *An. gambiae* complex. Our results demonstrate that testes are severely underdeveloped in hybrids between male *An. merus* and female *An. gambiae* or *An. coluzzii*. No meiotic chromosomes are identified in these hybrid males. However, testes have nearly normal morphologies and sizes but produce mostly

nonmotile spermatozoa in hybrids from the reciprocal crosses. Using chromosome X- and Y-specific fluorescent probes, we followed the process of meiosis in each species and their F1 hybrids between female *An. merus* and male *An. gambiae* or *An. coluzzii*. Unlike for pure species, sex chromosomes in meiotic prophase I of F1 hybrids are largely unpaired and all chromosomes show various degrees of insufficient condensation. Instead of entering the reductional division in meiosis I, primary spermatocytes undergo an equational mitotic division producing abnormal diploid sperm. Meiotic chromosomes of some F1 hybrid individuals are involved in *de novo* genome rearrangements. Yet, the germline-specific genes *β2-tubulin, Ams, mts*, and *Dzip1l* express normally in these hybrid males. Thus, our study identified cytogenetic errors in hybrids that arise during the early stages of postzygotic isolation. This knowledge will inform the development of innovative mosquito control strategies based on population suppression by manipulating reproduction via genetic technologies.

Author Summary

The genetic basis and molecular mechanisms of hybrid male sterility are of considerable interest as they inform our understanding of both speciation and normal fertility function. Studies of sterility in male hybrids between recently evolved species offer opportunities to identify developmental errors that arise early in speciation. We performed crosses between sibling species of the *Anopheles gambiae* complex to gain insights into a cellular basis of postzygotic isolation. We demonstrate that hybrid male sterility in the malaria mosquitoes is caused by two processes in reciprocal crosses: premeiotic arrest in germline stem cells and the failure of the reductional meiotic division in primary spermatocytes. The meiotic abnormalities also include unpairing of sex chromosomes, chromatin decompaction, and, in some cases, *de novo* genome

45 rearrangements. The failure of the reductional division in meiosis I results in the production of
46 diploid nonmotile sperm. Despite these meiotic errors, tested germline-specific genes express
47 normally in these hybrid males. Thus, our study identified cellular errors in hybrids that arise
48 during the early stages of postzygotic isolation. Studying molecular mechanisms of the
49 developmental abnormalities in testes of hybrids between closely related species of mosquitoes
50 will improve our knowledge of speciation and empower the sterile insect technique.
51

52 ## Introduction

53 Hybrid male fertility is among the first phenotypes affected as the postzygotic isolation between
54 species is being established [1]. Therefore, genetic factors, cellular basis, and molecular
55 mechanisms of hybrid male sterility are of considerable interest, as they inform our
56 understanding of both speciation and normal fertility function. Genetic loci responsible for
57 hybrid male sterility in plants and animals are often being identified using quantitative trait loci
58 (QTL) mapping [1-8]. In a variety of organisms, hybrid sterility can be caused by the genetic
59 factors on the X chromosome or by epistasis between X-linked and autosomal alleles [4, 8-15].
60 Studies in animals commonly assess testis shape, size or weight, as well as sperm morphology,
61 density or motility to define male sterility phenotypes. However, a cellular basis of hybrid male
62 sterility is rarely investigated. Cytological studies of spermatogenesis in sterile hybrids indicate
63 that multiple mechanisms of functional sterility are possible. Sterile hybrids between *Mus*
64 *musculus domesticus* and *M. m. musculus* have spermatogenic arrest in early meiosis I with
65 disrupted both homoeologous chromosome pairing and meiotic sex chromosome inactivation
66 [16, 17], as well as reductions in spermatocyte and spermatid number, increased apoptosis of
67 primary spermatocytes, and more multinucleated syncytia [18]. Studies of failed spermatogenesis

in different *Drosophila* hybrids observed arrests at the premeiotic stage [19], reduced chromosome pairing and unequal chromosome segregation in meiosis [20, 21], characteristic spermiogenic arrests [19], spermatid abnormalities [22], and problems in sperm bundling and motility [23, 24]. Detailed analyses of cellular and developmental abnormalities in testes of various hybrid organisms could help better define the causes of infertility. Cytological studies of spermatogenesis in hybrids may link different sterility phenotypes to the early or advance stages of postzygotic isolation. Moreover, identification of first-evolved cytogenetic errors in hybrids between closely related species could improve our understanding of speciation.

The *Anopheles gambiae* complex consists of at least eight morphologically nearly indistinguishable sibling species of African malaria mosquitoes [25, 26]. Genome-based estimations of the age of the *An. gambiae* complex vary from 1.85 [27] to as young as 0.526 million years [28]. Genomic introgression has been found prevalent in autosomal regions of several species indicating naturally occuring interspecies hybridization [27, 28]. Experimental crosses of species from the *An. gambiae* complex often produce sterile F1 hybrid males confirming Haldane's rule of sterility or inviability of the heterogametic sex [13, 29-31]. Early crossing experiments between members of the complex have found that hybrid male sterility is associated with various degrees of atrophies of testes and underdevelopment of sperms [30]. Examination of hybrid sterility in backcrosses of *An. gambiae* and *An. arabiensis* using an X-linked white-eye marker demonstrated a large effect of the X chromosome on male hybrid sterility [32]. The large X effect on hybrid sterility has been supported with a QTL mapping approach [13]. However, an introgression of the Y chromosome from *An. gambiae* into a background of *An. arabiensis* has shown no apparent influence on male fertility, fitness, or gene

91 expression [29]. A recent study of hybridization in nature has shown that postmating isolation is
92 positively associated with ecological divergence of *An. coluzzii, An. gambiae*, and *An. arabiensis*
93 [33]. However, the cellular basis and molecular mechanisms of hybrid male sterility in
94 mosquitoes are unknown. Because of the recent evolution and ease of hybridization, sibling
95 species of the *An. gambiae* complex offer great opportunities to provide insights into
96 mechanisms of speciation.
97
98 A recent World Health Organization report has shown that after a successful period of global
99 malaria control, progress has stalled since 2015. There are still 219 million cases and 435,000
100 related deaths from malaria without a tendency to decrease [34]. In the 60s-70s, the sterile insect
101 technique (SIT) was one of the first methods used to control the malaria-transmitting *Anopheles*
102 mosquitoes as it aimed to interfere with their reproduction by introducing sterile males into
103 natural populations. However, because of the low competitiveness of X-ray-irradiated males and
104 the lack of institutional commitments, the traditional SIT largely failed in controlling malaria
105 mosquitoes [35]. Novel genetic approaches based on CRISPR-Cas9 gene drives [36-40] show
106 potential toward the generation of self-sustainable and species-specific mosquito control
107 strategies. A better understanding of the normal male fertility function and mechanisms of
108 naturally occurring hybrid male sterility will inform the development of novel SIT tools and
109 implementation of pre-existing technologies for the control of malaria-transmitting mosquitoes.
110
111 Here, we investigate possible cellular causes of male sterility in hybrids between sibling species
112 of the *An. gambiae* complex. We asked three specific questions: (i) Which cellular processes are
113 involved in causing infertility in hybrid mosquito males? (ii) Are the defects leading to hybrid

male sterility premeiotic, meiotic, or postmeiotic? and (iii) What cytogenetic errors trigger the spermatogenic breakdown? We demonstrate that hybrid male sterility in malaria mosquitoes is caused by two cellular processes in reciprocal crosses: premeiotic arrest in germline stem cells and the failure of the reductional meiotic division in primary spermatocytes. Our data suggest that the meiotic abnormalities in hybrid males stem from the unpairing of the sex chromosomes and chromatin decondensation. Thus, our study identified first cytogenetic errors in hybrids that arise during the early stages of postzygotic isolation.

Results

Hybrid male sterility phenotypes at the cellular level

To obtain sterile males, we performed reciprocal crosses between *An. merus* MAF and *An. gambiae* ZANU or *An. coluzzii* MOPTI and MALI. Backcrossing of F1 males to parental females resulted in no progeny demonstrating sterility of F1 hybrid males. This result confirms Haldane's rule for the majority of interspecies crosses in the *An. gambiae* complex, except for crosses between *An. gambiae* and *An. coluzzii*: F1 females are fertile while F1 males are sterile [13, 29-31, 41, 42]. To investigate the developmental phenotypes associated with hybrid sterility, we dissected testes from adult males obtained from interspecies crosses and from pure species. Normal testes of pure species have a spindle-like shape (Fig 1A). We found obvious asymmetry in morphology and sizes of testes when reciprocal crosses were compared. Hybrid males from crosses between female *An. merus* and male *An. gambiae* or *An. coluzzii* display normal-like reproductive organs (Fig 1B). In contrast, F1 males from crosses between female *An. gambiae* or *An. coluzzii* and male *An. merus* show severely underdeveloped testes (Fig 1C). We then tested if

137 normal-like and underdeveloped testes of interspecies hybrids produce any sperm. In squashed
138 testes of 2-day-old adults of pure species, large amounts of mature spermatozoa with long tails
139 can be seen. After we crushed the testes, spermatozoa with vibrant motility escaped from the
140 ruptures (Fig 1A, S1 Movie). However, mature sperm or sperm motility hardly could be seen in
141 squashed or crushed normal-like testes of 2-day-old adult hybrids from crosses when *An. merus*
142 was the mother. Instead, we see delayed spermatid differentiation, fewer spermatids, and mostly
143 nonmotile spermatozoa with large heads and often two short tails growing from opposite ends of
144 the head (Fig 1B, S2 Movie). Only undifferentiated round cells could be seen in underdeveloped
145 testes of hybrids from reciprocal crosses when *An. merus* was the father (Fig 1C). Given the
146 small size of the degenerate testes, these round cells may represent germline stem cells. Thus,
147 neither normal-like nor underdeveloped testes of the interspecies hybrids produce mature motile
148 spermatozoa.
149
150 **The normal progress of meiosis in males of pure species**
151 Before we investigate meiosis of interspecies hybrids, we provide the first description of
152 chromosome behavior in meiosis of pure *Anopheles* species. The chromosome complement of
153 *Anopheles* males consists of three chromosome pairs: two autosomes (2 and 3) and X and Y sex
154 chromosomes. With the help of sex-chromosome-specific fluorescent probes, we followed the
155 progress of meiosis in *An. gambiae*, *An. coluzzii*, and *An. merus*. The following DNA sequences
156 were used as the probes for fluorescence *in situ* hybridization (FISH) (Table 1). Retroelement
157 *zanzibar* is specific to the Y chromosome of *An. gambiae* and *An. coluzzii* but is absent in *An.*
158 *merus*; 18S ribosomal DNA (rDNA) labels only the X chromosome in *An. gambiae* or *An.*
159 *coluzzii* but labels both X and Y chromosomes in *An. merus*; and satellite AgY53B [43] labels

160 both X and Y chromosomes in all three species [44]. Fig 2 shows normal activities of meiotic
161 chromosomes in testes of *An. gambiae* ZANU. In primary spermatocytes, all homologous
162 autosomes and sex chromosomes pair and display chiasmata in diplotene/diakinesis of prophase
163 I, they align with each other at the cell equator in metaphase I, and then move from each other in
164 anaphase I. In secondary spermatocytes, sister chromatids of each chromosome align with each
165 other at the cell equator in metaphase II and go to opposite poles of the cell during anaphase II.
166 Meiotic divisions produce spermatids that contain a haploid set of autosomes and either a Y or X
167 chromosome. *An. coluzzii* males show similar morphology and behavior of chromosomes during
168 meiosis (S1 Fig). Because retroelement *zanzibar* is absent in *An. merus*, we used satellite
169 AgY53B and 18S rDNA to label sex chromosomes in this species. Each of these probes
170 hybridized with both X and Y chromosomes in *An. merus*, making discrimination between X and
171 Y more difficult in this species. However, we could differentiate metaphase sex chromosomes by
172 the euchromatic arm of the X chromosome and by the slightly larger distal heterochromatic
173 block of the Y chromosome (S2 Fig). Heterochromatic parts of the X and Y chromosomes are
174 relatively large and structurally similar in *An. merus* in comparison with *An. gambiae* or *An.*
175 *coluzzii*. In the latter two species, the heterochromatic parts of the X and Y chromosomes are
176 relatively small and substantially different from each other both in size and genetic content [44].
177 Despite these differences between *An. merus* and either *An. gambiae* or *An. coluzzii*, the
178 activities of meiotic sex chromosomes in testes are similar in all three species.
179

180 **Table 1. Genomic sequences and primers used for FISH and RT-PCR.**

Name	GenBank ID	VectorBase ID	Forward and reverse primer sequences	Reference
18S rDNA	AM157179	AGAP028978	F: AACTGTGGAAAAGCCAGAGC	This study

			R: TCCACTTGATCCTTGCAAAA	
zanzibar	KP878482		F: TTCTTCGATGTTGTGCTGGA	[44]
			R: ATGGAGAAACAGGGCAACAA	
			F: TTGGCATTCATCTGTCCAAA	
			R: GCACCCTTGATCTCATGTCA	
AgY53B	AY754156		F: CCTTTAAACACATGCTCAAATT	[43]
			R: GTTTCTTCATCCTTAAAGCCTAG	
vasa	AY957503	AGAP008578	F: TTCTGCTGAGGTGCTTAGCG	This study
			R: CGTCTCCGCTCATGTTTCCT	
β2-tubulin	XM_314718	AGAP008622	F: GTACGTGCCGGATCATTTCG	This study
			R: GGCCAGTTTGCAAATGCACTA	
Ams	FJ869235	AGAP029148	F: CATACGGGAGGTGAGGAAAT	[45]
			R: CCCCTTCATGCTTCATCTT	
mts	FJ869236	AARA006451	F: TGGGATCCAAATTATTTCGTG	
			R: CTGTTCGGTTCAACAATGGA	
Dzip1l	FJ869237	AGAP001165	F: GGCCAAAGTGATACAAATTGTTT	
			R: CGTTTCCAATAGGGACTTCG	
AgS7	L20837	AGAP010592	F: AGAACCAGCAGACCACCATC	[46]
			R: GCTGCAAACTTCGGCTATTC	

Meiotic failures in F1 males of interspecies hybrids

To determine possible cytogenetic mechanisms of hybrid male sterility, we analyzed chromosome behavior in testes of hybrids from interspecies crosses. Meiotic chromosomes were present in normal-like testes of hybrids from the ♀*An. merus* × ♂*An. coluzzii/An. gambiae*

187 crosses and we identified important abnormalities of meiosis in these males (Fig 3). In primary
188 spermatocytes, homoeologous autosomes pair and form chiasmata in prophase I as in pure
189 species, but X and Y chromosomes do not display chiasmata in diplotene/diakinesis of prophase
190 I. We found this pattern consistent in all analyzed hybrid males. In hybrids, metaphase
191 chromosomes are visibly longer than at the same stage in pure species, indicating insufficient
192 chromatin condensation. Besides, homoeologous chromosomes in hybrids do not segregate
193 during anaphase. Instead, sister chromatids move to opposite poles of the dividing cell. Because
194 reductional division does not occur in hybrid males, both X and Y chromatids move to the same
195 pole during anaphase. As a result, haploid secondary spermatocytes do not form in these males.
196 Our FISH analysis demonstrated that each spermatid in testes of pure species normally contains
197 either an X or Y chromosome. In contrast, we found that both X and Y chromosomes present in
198 each spermatid of the hybrids (S3 Fig). Moreover, the abnormal spermatids are larger in size due
199 to insufficient chromatin condensation and the double chromosome content. Thus, we discovered
200 that chromosomes in normal-like testes of hybrid males start with a meiotic behavior in prophase
201 and then switch to a mitotic behavior in anaphase. The equational division of primary
202 spermatocytes results in dysfunctional diploid sperm in hybrids if *An. merus* is the mother. In
203 contrast, degenerate testes of F1s from the reciprocal ♀*An. coluzzii/gambiae* × ♂*An. merus*
204 crosses have only undifferentiated round germline stem cells. To visualize sex chromosomes, we
205 performed whole-mount FISH with labeled 18S rDNA and satellite AgY53B to mark the X
206 chromosomes of *An. coluzzii* and the Y chromosomes of *An. merus*, respectively (S4 Fig). Only
207 interphase sex chromosomes in nuclei of germline stem cells are detected indicating that meiosis
208 does not start in the underdeveloped testes of F1 hybrids if *An. merus* is the father. Thus, the
209 premeiotic arrest in the degenerate testes is the reason for the lack of spermatids in these hybrids.

Chromosomal and molecular abnormalities in interspecies hybrids

Here, we performed quantitative analyses of chromatin condensation and the X-Y chromosome pairing in pure species and their hybrids. We also tested if germline-specific genes express in sterile male hybrids from the reciprocal crosses. To determine the extent of chromatin condensation in normal-like testes of interspecies hybrids in comparison with pure species, we measured the lengths of metaphase chromosomes (S1 Table). The results of a statistical analysis with a two-sample pooled *t*-test show that chromosomes in F1 hybrids are typically longer than chromosomes in *An. coluzzii*, *An. gambiae*, or *An. merus* (Fig 4A, S5 Fig). For example, chromosomes of the *An. merus* origin in a hybrid background always show significant ($P<0.001$) elongation by at least 1.3 times in comparison with pure *An. merus*. The X chromosome of *An. merus* suffered the most serious undercondensation in hybrids exceeding the length of the X chromosome in the pure species background by 1.6-1.9-fold. Probably because the *An. merus* X is the longest chromosome in the hybrid karyotype, it can be subject to segregation delays during anaphase (S6 Fig), possibly causing slowing down of the cell division.

In our cytogenetic study of interspecies hybrids, the X and Y chromosomes do not show pairing or chiasmata in diplotene/diakinesis of prophase I (Fig 3). We hypothesized that sex chromosome pairing is affected in the early prophase I when individual chromosomes cannot be distinguished by direct visualization. To analyze the X-Y chromosome pairing at the pachytene stage of prophase I, we performed a whole-mount FISH and examined spatial positions of the X- and Y-specific fluorescent signals in confocal optical sections of nuclei in testes of pure species and their hybrids (S7 Fig). We recorded the number of nuclei with X and Y fluorescent signals

233 colocalized versus X and Y fluorescent signals located separately (Fig 4B). The results of a
234 statistical analysis with a two-sample pooled *t*-test demonstrate that X and Y chromosomes pair
235 in more than 90% of primary spermatocytes in the *An. coluzzii*, while they pair in less than 30%
236 of primary spermatocytes in F1 hybrids of ♀*An. merus* × ♂*An. coluzzii* (Fig 4C).
237
238 To test if premeiotic or meiotic failures are associated with the misexpression of germline-
239 specific genes, we analyzed the presence of the postmitotic germline transcripts *Ams, mts*, *Dzip1l*
240 [45], and *β2-tubulin* [47, 48] in F1 hybrid males (Table 1). The reverse transcription polymerase
241 chain reaction (RT-PCR) results show that these genes express at similar levels in the
242 reproductive tissues of *An. coluzzii* and F1 hybrids from the ♀*An. merus* × ♂*An. coluzzii* MOPTI
243 cross (Fig 4D). However, *Ams, mts*, *Dzip1l,* and *β2-tubulin* are strongly down regulated in
244 gonads of the ♀*An. coluzzii* MOPTI × ♂*An. merus* F1 hybrids, supporting our observation that
245 meiosis does not occur in these hybrids. In contrast, a pre-meiotic gene, *vasa* [49] (Table 1),
246 expresses at similar levels in reproductive tissues of all hybrids and pure species, indicating that
247 germline stem cells present even in degenerate testes of interspecies hybrids.
248
249 Besides the abnormalities that affect all progeny of the ♀*An. merus* × ♂*An. coluzzii/An. gambiae*
250 crosses, chromosomes of some hybrid individuals were involved in *de novo* genome
251 rearrangements (Fig 5). For example, a large fragment of the *An. merus* X chromosome,
252 including the rDNA locus, was translocated to the 2L arm of *An. coluzzii* in the male hybrid from
253 the ♀*An. merus* × ♂*An. coluzzii* MALI cross (Fig 5A). In addition, we detected a duplication of a
254 chromosomal segment involving the rDNA locus within the X chromosome of *An. merus* in the
255 ♀*An. merus* × ♂*An. gambiae* ZANU cross (Fig 5B). These rearrangements were not observed in

256 pure species, and their occurrence in F1 hybrid males suggests an increased genome instability as
257 a result of interspecies hybridization.
258

259 ## Discussion

260 ### Cellular and molecular phenotypes associated with hybrid male sterility

261 In this study, we performed the first detailed cytological analysis of spermatogenesis in pure
262 species and hybrids of mosquitoes. Hybrid male sterility phenotypes in the *An. gambiae* complex
263 are clearly asymmetric between the reciprocal crosses (Fig 6), as has been demonstrated earlier
264 for mosquitoes and other animals [8, 20, 30, 50]. The observed cellular and molecular
265 abnormalities suggest the following developmental scenarios in testes of the interspecies hybrids.
266 In hybrids from crosses with *An. merus* as the father, mitotic divisions of germline cells are
267 impaired, no meiosis occurred, and expression of postmitotic germline-specific genes is
268 repressed (Fig 4D). As a result, these hybrids have degenerate testes with arrested germline stem
269 cells. Degenerate testes have also been observed in F1 hybrids between sibling species of the *An.*
270 *albitarsis* [51] and the *An. barbirostris* [52] complexes. However, in hybrids from the reciprocal
271 crosses with *An. merus* as the mother, mitotic divisions of germ cells occur as normally as in
272 pure species. Moreover, germ cells in these hybrids go through meiotic prophase I as evidenced
273 from our cytogenetic analyses (Fig 3) and expression of the postmitotic germline genes (Fig 4D).
274 However, the downstream developmental processes in these hybrids are impaired. The
275 abnormalities begin in meiosis I where homoeologous chromosomes fail to segregate. Testes of
276 these hybrids show delayed spermatid differentiation, a smaller number of these cells, and
277 eventual formation of immotile abnormal (including two-tailed) sperm with insufficient
278 chromatin condensation (Fig 6). Thus, we demonstrate that premeiotic and meiotic failures

associate with hybrid male sterility in malaria mosquitoes. This observation is at odds with the commonly accepted view that more often hybrid males suffer postmeiotic sterility problems [1, 2]. Although many postmeiotic defects seen in *Drosophila* hybrids are indeed related to problems in sperm bundling and motility [2, 19, 23], some sperm abnormalities may stem from meiotic failures. For example, our results demonstrate that such sperm abnormalities as nonmotility, two-tailed heads, and chromatin decompaction in sperm heads result from the impaired meiosis I. However, very few studies have been devoted to the detailed cytological investigation of meiosis in interspecies hybrids, especially in dipteran insects. The closest studies to our own were performed by Theodosius Dobzhansky in 1933 and 1934, in which he described pronounced defects in meiosis I in sterile male hybrids from the ♀*D. pseudoobscura* × ♂*D. persimilis* cross [20, 21]. Also, a histological investigation of spermatogenesis in hybrid mice identified defects in meiosis I as a primary barrier to reproduction [18]. Additional studies of interspecies hybrids of various organisms should determine if the first meiotic division commonly fails when fertility is affected.

Cytogenetic mechanisms of hybrid male sterility

Our cytogenetic investigation of meiosis in pure *Anopheles* species revealed that the X and Y chromosomes normally pair tightly with each other throughout prophase I (Figs 2, 4BC, and S1, S2 Figs). Sex chromosomes in malaria mosquito males genetically recombine [44] highlighting an important difference from male meiosis in fruit flies [53-55]. As a result of the recombination, some mosquito species, such as *An. merus*, have homomorphic heterochromatic parts in their X and Y chromosomes (S2 Fig). Future sequencing and assembly of the heterochromatin in malaria

mosquitoes using long reads may yield important insights into structural and functional organization of the sex chromosomes, as it has been demonstrated for *Drosophila* [56].

Unlike pure species, the meiotic prophase I in F1 mosquito hybrids shows cytogenetic anomalies—low percentage of the X-Y chromosome pairing and insufficient chromatin condensation (Fig 7). Disruption of chromosome pairing and synapsis is frequently observed in interspecies hybrids of various organisms. Similar to the mosquitoes, pairing of X and Y chromosomes is more adversely affected than that of autosomes during the prophase I in male hybrids between Campbell's dwarf hamster and the Djungarian hamster [57]. A recent work has clarified that the autosomes of male hybrids between these hamster species undergo paring and recombination as normally as their parental forms do, but the heterochromatic arms of the X and Y chromosomes show a high frequency of asynapsis and recombination failure [58]. Another study has demonstrated a high rate of synaptic aberrations in multiple chromosomes of male hybrids between two chromosome races of the common shrew [59]. It has been proposed that asynapsis of heterospecific chromosomes in prophase I may provide a recurrently evolving trigger for the meiotic arrest of interspecific F1 hybrids of mice [8, 16]. Indeed, the presence of chiasmata and tension exerted across homologs ensures that yeast cells undergo reductional segregation [60]. Whenever it occurs, an asynapsis of chromosomes almost invariably triggers pachytene checkpoint and meiotic breakdown [61]. The genetic determinants of chromosome pairing and synapsis in both plants and animals are of great interest. In bread wheat, the *Ph1* locus has the largest effect on preventing homeologous pairing in meiosis [62]. In mice, a null mutation in the *PRDM9* gene causes chromosome asynapsis, arrest of spermatogenesis at pachynema, impairment of double-strand break repair, and disrupted sex-body formation [63].

The *PRDM9*-null phenotype resembles observed univalents and frequent X-Y dissociation in interspecies hybrids of mice [17]. A recent study has demonstrated a genetic link between meiotic recombination and hybrid male sterility [12]. It has been suggested that within species there may be selection to maintain sequence homozygosity for meiosis genes because their divergence can lead to reproductive isolation through failures of double-strand break formation and synapsis in hybrids [62].

It is possible that the absence of chiasmata between the X and Y chromosomes causes failure of reductional segregation in the mosquito hybrids. Unlike hybrids of mice, primary spermatocytes in the mosquito hybrids do not undergo arrest in meiosis I. Instead, they continue dividing by mitosis, in which sister chromatids move to the opposite poles of the dividing cell (Fig 7). This meiosis-mitosis switch is likely caused by the bi-orientation instead of the normal mono-orientation of sister kinetochores, in which tension across the centromere regions and proteins shugoshins plays a key role [53, 64, 65]. It is known that kinetochore-microtubules attachment errors are more commonly found in meiosis I than in mitosis [66, 67]. A mathematical model explains why kinetochore-microtubules attachment errors occur more frequently in the first meiotic division than in mitosis. The model suggests that the gradual increase of microtubules may help turn off the spindle assembly checkpoint in meiosis I leading to chromosome mis-segregation errors [68]. In mosquito hybrids, change in the orientation of sister kinetochores may be caused by reduced tension across the centromeres of homologous chromosomes due to chromatin decompaction. Changes in chromatin condensation have been documented in interspecies hybrids of diverse groups of organisms [69, 70]. In a study of F1 hybrids between *Arabidopsis thaliana* and *A. lyrata*, the *A. thaliana* chromatin became more compact, whereas

the *A. lyrata* chromatin became moderately less compact [70]. An intriguing spatial arrangement model suggests that that Y chromosome-linked variation may alter spatial position and packaging of other chromosomes in the nucleus [71]. Chromosome condensation and spatial position could also be affected in mosquito hybrids by improper function of condensins. A study of *Drosophila* male meiosis demonstrated that condensin II subunits, Cap-H2 and Cap-D3, are required to promote chromosome territory formation in primary spermatocyte nuclei. Moreover, anaphase I is abnormal in Cap-H2 mutants as chromatin bridges are formed between segregating heterologous and homologous chromosomes [72]. Thus, the interplay between the two phenotypes in mosquito hybrids—sex chromosome unpairing and chromatin decompaction—may result in failing a reductional meiotic division and proceeding to an equational mitotic division.

Evolution of spermatogenesis errors in interspecies hybrids

Reciprocal crosses in malaria mosquitoes and other organisms usually produce hybrids with sterility phenotypes of different degrees of severity [20, 30, 50]. This observation suggests that multiple stages of postzygotic isolation exist based on malfunction of the spermatogenesis. At the early stages of evolution, germline-specific genes still express normally and meiosis proceeds until metaphase I and then switches to an equational anaphase producing diploid sperm cells in hybrids. In this case, meiotic errors are characterized by the dramatically decreased pairing between sex chromosomes and insufficient chromatin condensation, which are seen in sterile hybrids from the ♀*An. merus* × ♂*An. coluzzii/An. gambiae* crosses (Figs 3, 7). The observed incidental chromosome rearrangements in mosquito hybrids (Fig 5) support the notion that genome instability is a common characteristic trait of hybrid incompatibility that may be

370 associated with increased transposable element activity, ectopic recombination, and double-
371 strand DNA breaks [73]. A recent work demonstrated that biogenesis of Piwi-interacting RNA
372 (piRNA) is enhanced in testes of hybrids between *Drosophila buzzatii* and *D. koepferae*. The
373 study argues that interspecies hybridization causes a genomic stress that can activate the piRNA
374 response pathway to counteract transposable element deregulation [74]. Because piRNAs
375 predominantly target long terminal repeats (LTR) retrotransposons in both *Anopheles* and
376 *Drosophila* [75], future studies of the piRNA expression in mosquito hybrids may identify
377 common and specific responses to the genomic stress in dipteran insect species. As species
378 continue to diverge, meiotic errors become more prominent, and new hybrid phenotypes appear
379 as has been seen, for example, in sterile male hybrids from the ♀*D. pseudoobscura* × ♂*D.*
380 *persimilis* cross [20, 21]. At this stage of postzygotic isolation, an abnormal anaphase is
381 characterized by unequal segregation of chromosomes resulting in spermatids with unbalanced
382 chromosome content. The more advanced interspecies divergence of meiosis is manifested by
383 the unpairing of the most chromosomes and by the malfunction of the abnormally elongated
384 spindle in sterile male hybrids [20, 21]. The next stage of evolution is spermatogenic arrest in
385 early meiosis I with disrupted homoeologous chromosome pairing, meiotic sex chromosome
386 inactivation, and increased apoptosis of spermatocytes as seen in mice hybrids [16-18].
387 Interestingly, chromosome unpairing and asynapsis in male hybrids stand out as common
388 spermatogenic phenotypes associated with sterility. It has been hypothesized that nongenic
389 repetitive sequences, as the fastest diverging component of the genome, may facilitate asynapsis
390 in hybrids, thus, representing suitable candidates for a Dobzhansky-Muller incompatibility [16].
391 Findings in *Drosophila* hybrids demonstrate that rapid evolution of heterochromatin may indeed
392 result in hybrid incompatibilities [69, 73, 76, 77]. Also, the centromere drive model has been

393 proposed to explain how paired chromosomes at meiosis I can be subject to nondisjunction
394 leading to infertility in *Drosophila* males [78, 79]. Accordingly, incompatibilities between
395 rapidly evolving centromeric components of emerging species, such as co-evolving the CENP-A
396 histone variant and its chaperone CAL1 [80], may account for species incompatibility between
397 centromeric histones and for postzygotic reproductive isolation. Finally, spermatogenic
398 abnormalities in hybrids can happen even before meiosis starts. A spermatogenic arrest at the
399 premeiotic stage is characterized by the repression of germline-specific genes and by the lack of
400 spermatocytes or spermatids in degenerate testes of hybrid males. These phenotypes have been
401 observed in sterile hybrids from the ♀*D. mauritiana* × ♂*D. sechellia* cross [19] and in sterile
402 hybrids from the ♀*An. coluzzii/An. gambiae* × ♂*An. merus* crosses (our study). Thus, cytological
403 analyses of spermatogenesis in interspecies hybrids can associate sterility phenotypes with early
404 or advance stages of speciation. Such studies of interspecies hybrids from diverse groups of
405 organisms may highlight general patterns and mechanisms in the origin and evolution of
406 postzygotic isolation.
407
408 **Conclusions**
409 Charles Darwin in the chapter "Hybridism" of his *Origin of Species* rightly argued that hybrid
410 sterility ‘‘is not a specially endowed quality, but is incidental on other acquired differences
411 [81].’’ Identification of the cellular and molecular differences acquired during the early stages of
412 postzygotic isolation between species is crucial to explaining both speciation and normal fertility
413 function. The cross between a female *An. merus* and a male *An. gambiae* or *An. coluzzii* produces
414 sterile hybrid males with spermatogenic abnormalities in the first meiotic division. Our study
415 uncovered differences in chromosome behaviors between pure *Anopheles* species and their

hybrids. The obtained data suggest that the meiotic abnormalities in hybrid males stem from the unpairing of the sex chromosomes and chromatin decondensation. Therefore, these malaria mosquitoes represent a great new system for studying a genetic basis and molecular mechanisms of species incompatibilities at early stages of postzygotic reproductive isolation.

Knowledge of the mechanisms of reproductive isolation in *Anopheles* has important implications not only for evolutionary biology but also for malaria control. The success of malaria transmission highly depends on the rate of mosquito reproduction. The development of novel approaches to control the reproductive output of mosquitoes must include the understanding of how fertility is regulated. Determining the mechanisms of sterility in male hybrids between closely related species of mosquitoes can also empower the sterile insect technique. In this respect, our results shed new light on the cellular processes and possible mechanisms in spermatogenesis that first appear when fertility is affected.

Materials and Methods

Mosquito maintenance and crossing experiments

The laboratory colonies of *An. gambiae* ZANU (MRA-594), *An. coluzzii* MOPTI (MRA-763), *An. coluzzii* MALI (MRA-860), and *An. merus* MAF (MRA-1156) were obtained from the Biodefense and Emerging Infections Research Resources Repository (BEI). Authentication of the species was performed by a cytogenetic analysis and by PCR diagnostics [82, 83]. Mosquitoes were reared at 27±1°C, with 12-hour photoperiod and 70±5% relative humidity. Larvae were fed fish food, and adult mosquitoes were fed 1% sugar water. To induce

439 oviposition, females were fed defibrinated sheep blood (Colorado Serum Co., Denver, Colorado,
440 USA) using artificial blood feeders. To perform interspecies crosses, male and female pupae
441 were separated to guarantee virginity of adult mosquitoes. We differentiated males and females
442 at the pupal stage using sex-specific differences in the shape of their terminalia [84]. After the
443 emergence of adults, crossing experiments were performed by combining 30 females and 15
444 males in one cage. Five days after random mating, the females were fed sheep blood. Two days
445 later, an egg dish, covered with moist filter paper to keep the eggs from drying out, was put into
446 the cage. Backcrosses of F1 males and parental females were done using a similar method. At
447 least two blood meals were fed to females with three repeats of each crosses.
448
449 **Male gonad and sperm observation**
450 Male gonads were dissected and photographed using an Olympus SZ 61 stereoscopy microscope
451 (Olympus, Tokyo, Japan) with an Olympus Q-Color 5 digital camera (Olympus, Tokyo, Japan).
452 We observed the testes of 30 males and took pictures of the testes of five males from each cross.
453 For sperm observation, testes were mounted in 20 µl sperm assay buffer containing 4 mM KCl,
454 1.3 mM $CaCl_2$, 145 mM NaCl, 5 mM D-glucose, 1 mM $MgCl_2$, and 10 mM 4-(2-hydroxyethyl)-
455 1-piperazineethanesulfonic acid (Hepes) [85]. After gently covering testes with a coverslip, they
456 were crushed, and sperm motility was observed under a phase contrast microscope BX 41
457 (Olympus, Tokyo, Japan). A Movie of sperm motility for at least five males of hybrids from each
458 cross and five males of pure species was recorded using a digital camera UC90 (Olympus,
459 Tokyo, Japan).
460
461 **Chromosome preparation**

462 Testes with male accessory glands were dissected from male pupae and 0-12 hours-old adults in
463 0.075% potassium chloride (KCl) hypotonic solution on a frosted glass slide (Thermo Fisher
464 Scientific, Waltham, MA, USA) under an Olympus SZ 61 dissecting microscope (Olympus,
465 Tokyo, Japan). To observe meiotic chromosomes, male accessory glands and other tissues were
466 removed, and only testes were left on the slide. Immediately after dissection, a drop of 50%
467 propionic acid was added to the testes, and they were covered with a 22×22-mm coverslip
468 (Thermo Fisher Scientific, Waltham, MA, USA). Preparations were tapped using the flat rubber
469 end of a pencil and observed under an Olympus CX41 phase-contrast microscope (Olympus,
470 Tokyo, Japan). The slides were frozen in liquid nitrogen, and a sharp razor was used to take off
471 the coverslips. The preparations were placed in 50% ethanol chilled at -20ºC for a minimum of 2
472 hours. Later, serial dehydrations were performed in 70%, 90%, and 100% ethanol for 5 min each
473 at room temperature (RT). Subsequently, the best preparations from at least 10 slides/individuals
474 with desired meiotic stages were chosen for further studies.
475
476 **DNA probe labeling and FISH**
477 Three DNA probes were used in this study: retroelement *zanzibar,* which is specific to the Y
478 chromosome of *An. gambiae* and *An. coluzzii*, 18S rDNA, which is specific to the X
479 chromosome of *An. gambiae* and *An. coluzzii* but labels both X and Y chromosomes of *An.*
480 *merus,* and satellite AgY53B, which labels X and Y chromosomes of all three species [44]. The
481 AgY53B satellite was amplified using primers that target the AgY53B/AgY477 satellite array
482 (Table 1). The probes were labeled by Cy3 or Cy5 fluorochromes using PCR with genomic DNA
483 as a template. Genomic DNA was extracted using DNeasy Blood & Tissue Kits (Qiagen, Hilden,
484 Germany) from virgin males of *An. gambiae* ZANU or *An. coluzzii* MOPTI for labeling

zanzibar, virgin males of *An. merus* MAF for labeling satellite AgY53B, and virgin females of *An. gambiae* or *An. coluzzii* for labeling 18S rDNA. Each 25 µl of a PCR mix consisted of 1-µl genomic DNA, 12.5-µl ImmoMix^{TM} 2x reaction mix (Bioline USA Inc., Taunton, MA, USA), 1 µl of 10-µM forward and reverse primers, and water. PCR labeling was performed in the Mastercycler® pro PCR thermocycler (Eppendorf, Hamburg, Germany) starting with a 95°C incubation for 10 min followed by 35 cycles of 95°C for 30 sec, 52°C for 30 sec, 72°C for 45 sec; 72°C for 5 min, and a final hold at 4°C. FISH was performed as previously described [86, 87]. Briefly, slides with good preparations were treated with 0.1-mg/ml RNase at 37℃ for 30 min. After washing with 2×SSC for 5 min twice, slides were digested with 0.01% pepsin and 0.037% HCl solution for 5 min at 37°C. After washing slides in 1×PBS for 5 min at RT two times, preparations were fixed in 3.7% formaldehyde for 10 min at RT. Slides were then washed in 1×PBS and dehydrated in a series of 70%, 80%, and 100% ethanol for 5 min at RT. Then 10 µl of probes were mixed, added to the preparations, and incubated at 37℃ overnight. After washing slides in 1×SSC at 60℃ for 5 min, 4×SSC/NP40 solution at 37℃ for 10 min, and 1×PBS for 5 min at RT, preparations were counterstained with a DAPI-antifade solution (Life Technologies, Carlsbad, CA, USA) and kept in the dark for at least 2 hours before visualization with a fluorescent microscope.

Cytogenetic analyses

Cytogenetic analyses of meiotic and mitotic stages and of behaviors of FISH-labeled chromosomes were performed on at least 10 male individuals of each pure species and of each hybrid. To visualize and photograph meiotic chromosomes after FISH, we used an Olympus BX61 microscope (Olympus, Tokyo, Japan) with a connected camera Olympus U-CMAD3

(Olympus, Tokyo, Japan). Lengths of well-spread 10 metaphase I chromosomes of each species and of each hybrid were measured using the ruler tool in Adobe Photoshop CS6 (Adobe Inc., San Jose, CA, USA). Since the variances for both groups were equal, a statistical two-sample pooled *t*-test was done with the JMP 13 software (SAS Institute Inc., Cary, NC, USA).

Whole-mount FISH and analysis of chromosome pairing

Testes from one-day-old adults of pure species and hybrids were dissected in 1×PBS solution and fixed in 3.7% paraformaldehyde in 1×PBS with 0.1% tween-20 (PBST) for 10 min at room temperature. After incubation with 0.1-mg/ml RNase for 30 min at 37 ºC, testes were penetrated with 1% triton/0.1M HCl in PBST for 10 min at room temperature. After adding labeled DNA probes, testes were incubated at 75 ºC for 5 min (denaturation) and 37 ºC overnight (hybridization). Later, testes were washed with 2×SSC and mounted with a DAPI-antifade solution (Life Technologies, Carlsbad, CA, USA). Testes from 6 individuals of pure species and of hybrids were scanned and analyzed. Visualization and z-tack 3D scanning were performed on the whole testes with an interval of 1.25 μm between two optical sections under a 63× oil lens of Zeiss LSM 880 confocal laser scanning microscope (Carl Zeiss AG, Oberkochen, Germany). Based on the size of the testis cells and on the limitations of microscope imaging, we chose from the first to sixteenth optical layers with strong and clearly detected fluorescent signals to analyze sex-chromosome-pairing events. Specifically, cell nuclei at the early stages of meiotic prophase I from 4^{th}±1, 8^{th}±1, and 12^{th}±1 optical layers were used to count paring events. A total of 418 and 489 nuclei at the early stages of meiotic prophase I were analyzed for paring and unpairing of the sex chromosomes in pure species and hybrids, respectively (S2 Table). The percentage of the numbers of cells with pairing and no paring of sex chromosomes was used to compare parental

531 species and hybrids. Since the variances for both groups were equal, a statistical two-sample
532 pooled *t*-test was done using the JMP 13 software (SAS Institute Inc., Cary, NC, USA).
533
534 **RNA extraction and RT-PCR**
535 RNA was extracted from 40 abdomens (only distal segments that include testes) and from 20
536 carcasses of 1- to 2-day-old virgin adult males of *An. coluzzii* MOPTI, as well as of interspecies
537 hybrids from crosses ♀*An. coluzzii* MOPTI × ♂*An. merus* and ♀*An. merus* × ♂*An. coluzzii*
538 MOPTI using a Direct-Zol™ RNA MiniPrep Kit (Zymo Research, Irvine, California, US).
539 cDNA for selected genes (Table 1) was generated in a 40-µl reaction that contained 8 µl of 5×
540 first-strand buffer, 4 µl of 0.1-M dithiothreitol (DTT), 2 µl of 50-µM random hexamer primer
541 (Thermo Fisher Scientific, Waltham, MA, USA), 1 µl of 25-mM dNTP mix solution (Thermo
542 Fisher Scientific, Waltham, MA, USA), 1 µl of 40-U/µl RNAsin (Promega, Madison, WI, USA),
543 2 µl of 200-U/µl M-MLV Reverse Transcriptase (Thermo Fisher Scientific, Waltham, MA,
544 USA), 1ng to 2µg of RNA and water. After incubation at 42°C for 1h, the reaction was stopped
545 by incubation at 95°C for 5 min. Two-step RT-PCR was performed to analyze the gene
546 expression. Each 25-µl PCR mix consisted of 1-µl cDNA, 12.5-µl ImmoMix™ 2× reaction-mix
547 (Bioline USA Inc., Taunton, MA, USA), 1 µl of 10-µM forward and reverse primers, and water.
548 PCR was performed in the Mastercycler® pro PCR thermocycler (Eppendorf, Hamburg,
549 Germany) starting with a 95°C incubation for 10 min followed by 35 cycles of 95°C for 30 sec,
550 57°C for 30 sec, 72°C for 30 sec; 72°C for 10 min; and a final hold at 4°C. Amplification
551 products were visualized in a 1-1.5% agarose gel.
552
553 **Acknowledgments**

We thank the Malaria Research and Reference Reagent Resource (MR4) at the BEI for providing us the laboratory colonies of malaria mosquitoes and Melissa Wade for proofreading the text.

References

1. Powell JR. Progress and Prospects in Evolutionary Biology. New York - Oxford: Oxford University Press; 1997. 562 p.

2. Coyne JA, Orr HA. Speciation. Sunderland, Mass.: Sinauer Associates; 2004. xiii, 545, 2 pages of plates p.

3. Larson EL, VaLnderpool D, Sarver BAJ, Callahan C, Keeble S, Provencio LL, et al. The Evolution of Polymorphic Hybrid Incompatibilities in House Mice. Genetics. 2018;209(3):845-59. Epub 2018/04/26. doi: 10.1534/genetics.118.300840. PubMed PMID: 29692350; PubMed Central PMCID: PMCPMC6028243.

4. Good JM, Dean MD, Nachman MW. A complex genetic basis to X-linked hybrid male sterility between two species of house mice. Genetics. 2008;179(4):2213-28. Epub 2008/08/12. doi: 10.1534/genetics.107.085340. PubMed PMID: 18689897; PubMed Central PMCID: PMCPMC2516092.

5. White MA, Stubbings M, Dumont BL, Payseur BA. Genetics and evolution of hybrid male sterility in house mice. Genetics. 2012;191(3):917-34. Epub 2012/05/05. doi: 10.1534/genetics.112.140251. PubMed PMID: 22554891; PubMed Central PMCID: PMCPMC3389984.

6. Fishman L, Stathos A, Beardsley PM, Williams CF, Hill JP. Chromosomal rearrangements and the genetics of reproductive barriers in mimulus (monkey flowers).

576 Evolution. 2013;67(9):2547-60. Epub 2013/09/17. doi: 10.1111/evo.12154. PubMed PMID:
577 24033166.
578 7. Leppala J, Savolainen O. Nuclear-cytoplasmic interactions reduce male fertility in
579 hybrids of Arabidopsis lyrata subspecies. Evolution. 2011;65(10):2959-72. Epub 2011/10/05.
580 doi: 10.1111/j.1558-5646.2011.01361.x. PubMed PMID: 21967435.
581 8. Bhattacharyya T, Reifova R, Gregorova S, Simecek P, Gergelits V, Mistrik M, et al. X
582 chromosome control of meiotic chromosome synapsis in mouse inter-subspecific hybrids. PLoS
583 Genet. 2014;10(2):e1004088. Epub 2014/02/12. doi: 10.1371/journal.pgen.1004088. PubMed
584 PMID: 24516397; PubMed Central PMCID: PMCPMC3916230.
585 9. Dobzhansky T. Studies on Hybrid Sterility. II. Localization of Sterility Factors in
586 Drosophila Pseudoobscura Hybrids. Genetics. 1936;21(2):113-35. Epub 1936/03/01. PubMed
587 PMID: 17246786; PubMed Central PMCID: PMCPMC1208664.
588 10. Turissini DA, Liu G, David JR, Matute DR. The evolution of reproductive isolation in the
589 Drosophila yakuba complex of species. J Evol Biol. 2015;28(3):557-75. Epub 2015/01/23. doi:
590 10.1111/jeb.12588. PubMed PMID: 25611516.
591 11. Hu XS, Filatov DA. The large-X effect in plants: increased species divergence and
592 reduced gene flow on the Silene X-chromosome. Mol Ecol. 2016;25(11):2609-19. Epub
593 2015/10/20. doi: 10.1111/mec.13427. PubMed PMID: 26479725.
594 12. Balcova M, Faltusova B, Gergelits V, Bhattacharyya T, Mihola O, Trachtulec Z, et al.
595 Hybrid Sterility Locus on Chromosome X Controls Meiotic Recombination Rate in Mouse.
596 PLoS Genet. 2016;12(4):e1005906. Epub 2016/04/23. doi: 10.1371/journal.pgen.1005906.
597 PubMed PMID: 27104744; PubMed Central PMCID: PMCPMC4841592.

598 13. Slotman M, Della Torre A, Powell JR. The genetics of inviability and male sterility in
599 hybrids between Anopheles gambiae and An. arabiensis. Genetics. 2004;167(1):275-87. Epub
600 2004/05/29. doi: 167/1/275 [pii]. PubMed PMID: 15166154; PubMed Central PMCID:
601 PMC1470845.
602 14. Phadnis N, Orr HA. A Single Gene Causes Both Male Sterility and Segregation
603 Distortion in Drosophila Hybrids. Science. 2009;323(5912):376-9. doi:
604 10.1126/science.1163934. PubMed PMID: WOS:000262481400037.
605 15. Ting CT, Tsaur SC, Wu ML, Wu CI. A rapidly evolving homeobox at the site of a hybrid
606 sterility gene. Science. 1998;282(5393):1501-4. doi: DOI 10.1126/science.282.5393.1501.
607 PubMed PMID: WOS:000077110800058.
608 16. Bhattacharyya T, Gregorova S, Mihola O, Anger M, Sebestova J, Denny P, et al.
609 Mechanistic basis of infertility of mouse intersubspecific hybrids. Proc Natl Acad Sci U S A.
610 2013;110(6):E468-77. Epub 2013/01/19. doi: 10.1073/pnas.1219126110. PubMed PMID:
611 23329330; PubMed Central PMCID: PMCPMC3568299.
612 17. Forejt J, Ivanyi P. Genetic studies on male sterility of hybrids between laboratory and
613 wild mice (Mus musculus L.). Genet Res. 1974;24(2):189-206. Epub 1974/10/01. PubMed
614 PMID: 4452481.
615 18. Schwahn DJ, Wang RJ, White MA, Payseur BA. Genetic Dissection of Hybrid Male
616 Sterility Across Stages of Spermatogenesis. Genetics. 2018. Epub 2018/10/20. doi:
617 10.1534/genetics.118.301658. PubMed PMID: 30333190.
618 19. Kulathinal R, Singh RS. Cytological Characterization of Premeiotic Versus Postmeiotic
619 Defects Producing Hybrid Male Sterility among Sibling Species of the Drosophila Melanogaster

620 Complex. Evolution. 1998;52(4):1067-79. Epub 1998/08/01. doi: 10.1111/j.1558-
621 5646.1998.tb01834.x. PubMed PMID: 28565214.
622 20. Dobzhansky T. Studies on hybrid sterility. I. Spermatogenesis in pure and hybrid
623 Drosophila pseudoobscura. ZEITSCHR ZELLJORSCH U MIKROSK ANAT. 1934;21(2):169-
624 223.
625 21. Dobzhansky T. On the sterility of the interracial hybrids in Drosophila pseudoobscura. P
626 Natl Acad Sci USA. 1933;19:397-403. doi: DOI 10.1073/pnas.19.4.397. PubMed PMID:
627 WOS:000201970900068.
628 22. Hardy RW, Lougheed A, Markow TA. Reproductive tract and spermatid abnormalities of
629 hybrid males from reciprocal crosses between Drosophila mojavensis and D. arizonae. Fly
630 (Austin). 2011;5(2):76-80. Epub 2011/05/05. doi: 10.4161/fly.5.2.15571. PubMed PMID:
631 21540637.
632 23. Coyne JA. Genetic-Basis of Male-Sterility in Hybrids between 2 Closely Related Species
633 of Drosophila. P Natl Acad Sci-Biol. 1984;81(14):4444-7. doi: DOI 10.1073/pnas.81.14.4444.
634 PubMed PMID: WOS:A1984TD00100044.
635 24. Masly JP, Jones CD, Noor MA, Locke J, Orr HA. Gene transposition as a cause of hybrid
636 sterility in Drosophila. Science. 2006;313(5792):1448-50. Epub 2006/09/09. doi:
637 10.1126/science.1128721. PubMed PMID: 16960009.
638 25. Coluzzi M, Sabatini A, della Torre A, Di Deco MA, Petrarca V. A polytene chromosome
639 analysis of the Anopheles gambiae species complex. Science. 2002;298(5597):1415-8. PubMed
640 PMID: 12364623.
641 26. Coetzee M, Hunt RH, Wilkerson R, Della Torre A, Coulibaly MB, Besansky NJ.
642 Anopheles coluzzii and Anopheles amharicus, new members of the Anopheles gambiae

643 complex. Zootaxa. 2013;3619(3):246-74. doi: Doi 10.11646/Zootaxa.3619.3.2. PubMed PMID:
644 ISI:000315436200002.
645 27. Fontaine MC, Pease JB, Steele A, Waterhouse RM, Neafsey DE, Sharakhov IV, et al.
646 Extensive introgression in a malaria vector species complex revealed by phylogenomics.
647 Science. 2015;347(6217):42-+. doi: Unsp 1258524
648 Doi 10.1126/Science.1258524. PubMed PMID: WOS:000347102300041.
649 28. Thawornwattana Y, Dalquen D, Yang Z. Coalescent Analysis of Phylogenomic Data
650 Confidently Resolves the Species Relationships in the Anopheles gambiae Species Complex.
651 Mol Biol Evol. 2018;35(10):2512-27. Epub 2018/08/14. doi: 10.1093/molbev/msy158. PubMed
652 PMID: 30102363; PubMed Central PMCID: PMCPMC6188554.
653 29. Bernardini F, Galizi R, Wunderlich M, Taxiarchi C, Kranjc N, Kyrou K, et al. Cross-
654 Species Y Chromosome Function Between Malaria Vectors of the Anopheles gambiae Species
655 Complex. Genetics. 2017;207(2):729-40. Epub 2017/09/02. doi: 10.1534/genetics.117.300221.
656 PubMed PMID: 28860320; PubMed Central PMCID: PMCPMC5629335.
657 30. Davidson G, Paterson HE, Coluzzi M, Mason GF, Micks DW. The Anopheles gambiae
658 Complex. In: Wright JW, Pal R, editors. Genetics of Insect Vectors of Diesease. Amsterdam-
659 London-New York: Elsevier Publishing Company; 1967. p. 211-49.
660 31. Presgraves DC, Orr HA. Haldane's rule in taxa lacking a hemizygous X. Science.
661 1998;282(5390):952-4. Epub 1998/10/30. PubMed PMID: 9794768.
662 32. Curtis CF. The mechanism of hybrid male sterility from crosses in the Anopheles
663 gambiae and Glossina morsitans complexes. In: Steiner WM, Tabachnick WJ, Rai KS, Narang S,
664 editors. Recent Developments in the Genetics of Disease Vectors. Champaign, IL: Stipes
665 Publishing Company; 1982. p. 290-312.

666 33. Pombi M, Kengne P, Gimonneau G, Tene-Fossog B, Ayala D, Kamdem C, et al.
667 Dissecting functional components of reproductive isolation among closely related sympatric
668 species of the Anopheles gambiae complex. Evol Appl. 2017;10(10):1102-20. Epub 2017/11/21.
669 doi: 10.1111/eva.12517. PubMed PMID: 29151864; PubMed Central PMCID:
670 PMCPMC5680640.
671 34. World malaria report. Geneva, Switzerland: World Health Organization, 2018.
672 35. Dame DA, Curtis CF, Benedict MQ, Robinson AS, Knols BG. Historical applications of
673 induced sterilisation in field populations of mosquitoes. Malar J. 2009;8 Suppl 2:S2. Epub
674 2009/12/16. doi: 10.1186/1475-2875-8-S2-S2. PubMed PMID: 19917072; PubMed Central
675 PMCID: PMCPMC2777324.
676 36. Hammond A, Galizi R, Kyrou K, Simoni A, Siniscalchi C, Katsanos D, et al. A CRISPR-
677 Cas9 gene drive system targeting female reproduction in the malaria mosquito vector Anopheles
678 gambiae. Nat Biotechnol. 2016;34(1):78-83. Epub 2015/12/08. doi: 10.1038/nbt.3439. PubMed
679 PMID: 26641531; PubMed Central PMCID: PMCPMC4913862.
680 37. Macias VM, Ohm JR, Rasgon JL. Gene Drive for Mosquito Control: Where Did It Come
681 from and Where Are We Headed? Int J Env Res Pub He. 2017;14(9). doi: ARTN 1006
682 10.3390/ijerph14091006. PubMed PMID: WOS:000411574400058.
683 38. Kyrou K, Hammond AM, Galizi R, Kranjc N, Burt A, Beaghton AK, et al. A CRISPR-
684 Cas9 gene drive targeting doublesex causes complete population suppression in caged Anopheles
685 gambiae mosquitoes. Nat Biotechnol. 2018;36(11):1062-6. Epub 2018/09/25. doi:
686 10.1038/nbt.4245. PubMed PMID: 30247490.
687 39. Gantz VM, Jasinskiene N, Tatarenkova O, Fazekas A, Macias VM, Bier E, et al. Highly
688 efficient Cas9-mediated gene drive for population modification of the malaria vector mosquito

689 Anopheles stephensi. Proc Natl Acad Sci U S A. 2015;112(49):E6736-43. Epub 2015/11/26. doi:
690 10.1073/pnas.1521077112. PubMed PMID: 26598698; PubMed Central PMCID:
691 PMCPMC4679060.
692 40. Hammond AM, Kyrou K, Bruttini M, North A, Galizi R, Karlsson X, et al. The creation
693 and selection of mutations resistant to a gene drive over multiple generations in the malaria
694 mosquito. PLoS Genet. 2017;13(10):e1007039. Epub 2017/10/05. doi:
695 10.1371/journal.pgen.1007039. PubMed PMID: 28976972; PubMed Central PMCID:
696 PMCPMC5648257.
697 41. Diabate A, Dabire RK, Millogo N, Lehmann T. Evaluating the effect of postmating
698 isolation between molecular forms of Anopheles gambiae (Diptera: Culicidae). J Med Entomol.
699 2007;44(1):60-4. Epub 2007/02/14. PubMed PMID: 17294921.
700 42. Aboagye-Antwi F, Alhafez N, Weedall GD, Brothwood J, Kandola S, Paton D, et al.
701 Experimental swap of Anopheles gambiae's assortative mating preferences demonstrates key role
702 of X-chromosome divergence island in incipient sympatric speciation. PLoS Genet.
703 2015;11(4):e1005141. Epub 2015/04/17. doi: 10.1371/journal.pgen.1005141. PubMed PMID:
704 25880677; PubMed Central PMCID: PMCPMC4400153.
705 43. Krzywinski J, Sangare D, Besansky NJ. Satellite DNA from the Y chromosome of the
706 malaria vector Anopheles gambiae. Genetics. 2005;169(1):185-96. Epub 2004/10/07. doi:
707 genetics.104.034264 [pii]
708 10.1534/genetics.104.034264. PubMed PMID: 15466420; PubMed Central PMCID:
709 PMC1448884.
710 44. Hall AB, Papathanos PA, Sharma A, Cheng C, Akbari OS, Assour L, et al. Radical
711 remodeling of the Y chromosome in a recent radiation of malaria mosquitoes. Proc Natl Acad

712 Sci U S A. 2016;113(15):E2114-23. doi: 10.1073/pnas.1525164113. PubMed PMID: 27035980;
713 PubMed Central PMCID: PMCPMC4839409.
714 45. Krzywinska E, Krzywinski J. Analysis of expression in the Anopheles gambiae
715 developing testes reveals rapidly evolving lineage-specific genes in mosquitoes. BMC
716 Genomics. 2009;10:300. Epub 2009/07/08. doi: 10.1186/1471-2164-10-300. PubMed PMID:
717 19580678; PubMed Central PMCID: PMC2713267.
718 46. Balabanidou V, Kampouraki A, MacLean M, Blomquist GJ, Tittiger C, Juarez MP, et al.
719 Cytochrome P450 associated with insecticide resistance catalyzes cuticular hydrocarbon
720 production in Anopheles gambiae. Proc Natl Acad Sci U S A. 2016;113(33):9268-73. Epub
721 2016/07/22. doi: 10.1073/pnas.1608295113. PubMed PMID: 27439866; PubMed Central
722 PMCID: PMCPMC4995928.
723 47. Catteruccia F, Crisanti A, Wimmer EA. Transgenic technologies to induce sterility.
724 Malar J. 2009;8 Suppl 2:S7. Epub 2009/12/16. doi: 10.1186/1475-2875-8-S2-S7. PubMed
725 PMID: 19917077; PubMed Central PMCID: PMCPMC2777329.
726 48. Kemphues KJ, Kaufman TC, Raff RA, Raff EC. The testis-specific beta-tubulin subunit
727 in Drosophila melanogaster has multiple functions in spermatogenesis. Cell. 1982;31(3 Pt
728 2):655-70. Epub 1982/12/01. PubMed PMID: 6819086.
729 49. Papathanos PA, Windbichler N, Menichelli M, Burt A, Crisanti A. The vasa regulatory
730 region mediates germline expression and maternal transmission of proteins in the malaria
731 mosquito Anopheles gambiae: a versatile tool for genetic control strategies. BMC Mol Biol.
732 2009;10:65. Epub 2009/07/04. doi: 10.1186/1471-2199-10-65. PubMed PMID: 19573226;
733 PubMed Central PMCID: PMCPMC2713240.

734 50. Good JM, Handel MA, Nachman MW. Asymmetry and polymorphism of hybrid male
735 sterility during the early stages of speciation in house mice. Evolution. 2008;62(1):50-65. Epub
736 2007/11/17. doi: 10.1111/j.1558-5646.2007.00257.x. PubMed PMID: 18005156; PubMed
737 Central PMCID: PMCPMC2907743.
738 51. Fontoura NG, Araki AS, Azevedo RV, Galardo AKR, Peixoto AA, Lima JBP. Hybrid
739 sterility in crosses between two Brazilian sibling species of the Anopheles albitarsis complex.
740 Parasite Vector. 2014;7. doi: ARTN 559

741 10.1186/s13071-014-0559-6. PubMed PMID: WOS:000348945100001.
742 52. Suwannamit S, Baimai V, Otsuka Y, Saeung A, Thongsahuan S, Tuetun B, et al.
743 Cytogenetic and molecular evidence for an additional new species within the taxon Anopheles
744 barbirostris (Diptera: Culicidae) in Thailand. Parasitol Res. 2009;104(4):905-18. Epub
745 2008/12/02. doi: 10.1007/s00436-008-1272-1. PubMed PMID: 19043741.
746 53. McKee BD, Yan R, Tsai JH. Meiosis in male Drosophila. Spermatogenesis.
747 2012;2(3):167-84. Epub 2012/10/23. doi: 10.4161/spmg.21800. PubMed PMID: 23087836;
748 PubMed Central PMCID: PMCPMC3469440.
749 54. Bonaccorsi S, Gatti M. Drosophila Male Meiosis. Methods Mol Biol. 2017;1471:277-88.
750 Epub 2017/03/30. doi: 10.1007/978-1-4939-6340-9_16. PubMed PMID: 28349403.
751 55. Hawley RS. Meiosis: How male flies do meiosis. Current Biology. 2002;12(19):R660-
752 R2. doi: Doi 10.1016/S0960-9822(02)01161-2. PubMed PMID: WOS:000178404100010.
753 56. Chang CH, Larracuente AM. Heterochromatin-Enriched Assemblies Reveal the
754 Sequence and Organization of the Drosophila melanogaster Y Chromosome. Genetics. 2018.
755 Epub 2018/11/14. doi: 10.1534/genetics.118.301765. PubMed PMID: 30420487.

756 57. Ishishita S, Tsuboi K, Ohishi N, Tsuchiya K, Matsuda Y. Abnormal pairing of X and Y
757 sex chromosomes during meiosis I in interspecific hybrids of Phodopus campbelli and P.
758 sungorus. Sci Rep. 2015;5:9435. Epub 2015/03/25. doi: 10.1038/srep09435. PubMed PMID:
759 25801302; PubMed Central PMCID: PMCPMC4371188.
760 58. Bikchurina TI, Tishakova KV, Kizilova EA, Romanenko SA, Serdyukova NA,
761 Torgasheva AA, et al. Chromosome Synapsis and Recombination in Male-Sterile and Female-
762 Fertile Interspecies Hybrids of the Dwarf Hamsters (Phodopus, Cricetidae). Genes (Basel).
763 2018;9(5). Epub 2018/04/26. doi: 10.3390/genes9050227. PubMed PMID: 29693587; PubMed
764 Central PMCID: PMCPMC5977167.
765 59. Belonogova NM, Polyakov AV, Karamysheva TV, Torgasheva AA, Searle JB, Borodin
766 PM. Chromosome Synapsis and Recombination in Male Hybrids between Two Chromosome
767 Races of the Common Shrew (Sorex araneus L., Soricidae, Eulipotyphla). Genes (Basel).
768 2017;8(10). Epub 2017/10/21. doi: 10.3390/genes8100282. PubMed PMID: 29053571; PubMed
769 Central PMCID: PMCPMC5664132.
770 60. Miyazaki S, Kim J, Sakuno T, Watanabe Y. Hierarchical Regulation of Centromeric
771 Cohesion Protection by Meikin and Shugoshin during Meiosis I. Cold Spring Harb Symp Quant
772 Biol. 2017;82:259-66. Epub 2017/12/03. doi: 10.1101/sqb.2017.82.033811. PubMed PMID:
773 29196561.
774 61. Bolcun-Filas E, Schimenti JC. Genetics of meiosis and recombination in mice. Int Rev
775 Cell Mol Biol. 2012;298:179-227. Epub 2012/08/11. doi: 10.1016/B978-0-12-394309-5.00005-
776 5. PubMed PMID: 22878107.

777 62. Bomblies K, Higgins JD, Yant L. Meiosis evolves: adaptation to external and internal
778 environments. New Phytol. 2015;208(2):306-23. Epub 2015/06/16. doi: 10.1111/nph.13499.
779 PubMed PMID: 26075313.
780 63. Hayashi K, Yoshida K, Matsui Y. A histone H3 methyltransferase controls epigenetic
781 events required for meiotic prophase. Nature. 2005;438(7066):374-8. Epub 2005/11/18. doi:
782 10.1038/nature04112. PubMed PMID: 16292313.
783 64. Gutierrez-Caballero C, Cebollero LR, Pendas AM. Shugoshins: from protectors of
784 cohesion to versatile adaptors at the centromere. Trends Genet. 2012;28(7):351-60. Epub
785 2012/05/01. doi: 10.1016/j.tig.2012.03.003. PubMed PMID: 22542109.
786 65. Pinto BS, Orr-Weaver TL. Drosophila protein phosphatases 2A B' Wdb and Wrd regulate
787 meiotic centromere localization and function of the MEI-S332 Shugoshin. Proc Natl Acad Sci U
788 S A. 2017;114(49):12988-93. Epub 2017/11/22. doi: 10.1073/pnas.1718450114. PubMed PMID:
789 29158400; PubMed Central PMCID: PMCPMC5724294.
790 66. Kitajima TS, Ohsugi M, Ellenberg J. Complete kinetochore tracking reveals error-prone
791 homologous chromosome biorientation in mammalian oocytes. Cell. 2011;146(4):568-81. Epub
792 2011/08/23. doi: 10.1016/j.cell.2011.07.031. PubMed PMID: 21854982.
793 67. Jones KT, Lane SI. Molecular causes of aneuploidy in mammalian eggs. Development.
794 2013;140(18):3719-30. Epub 2013/08/29. doi: 10.1242/dev.090589. PubMed PMID: 23981655.
795 68. Saka Y, Giuraniuc CV, Ohkura H. Accurate chromosome segregation by probabilistic
796 self-organisation. Bmc Biol. 2015;13:65. Epub 2015/08/13. doi: 10.1186/s12915-015-0172-y.
797 PubMed PMID: 26264961; PubMed Central PMCID: PMCPMC4533937.
798 69. Blum JA, Bonaccorsi S, Marzullo M, Palumbo V, Yamashita YM, Barbash DA, et al.
799 The Hybrid Incompatibility Genes Lhr and Hmr Are Required for Sister Chromatid Detachment

During Anaphase but Not for Centromere Function. Genetics. 2017;207(4):1457-72. Epub 2017/10/20. doi: 10.1534/genetics.117.300390. PubMed PMID: 29046402; PubMed Central PMCID: PMCPMC5714459.

70. Zhu W, Hu B, Becker C, Dogan ES, Berendzen KW, Weigel D, et al. Altered chromatin compaction and histone methylation drive non-additive gene expression in an interspecific Arabidopsis hybrid. Genome Biol. 2017;18(1):157. Epub 2017/08/24. doi: 10.1186/s13059-017-1281-4. PubMed PMID: 28830561; PubMed Central PMCID: PMCPMC5568265.

71. Francisco FO, Lemos B. How do y-chromosomes modulate genome-wide epigenetic States: genome folding, chromatin sinks, and gene expression. J Genomics. 2014;2:94-103. Epub 2014/07/25. doi: 10.7150/jgen.8043. PubMed PMID: 25057325; PubMed Central PMCID: PMCPMC4105431.

72. Hartl TA, Sweeney SJ, Knepler PJ, Bosco G. Condensin II resolves chromosomal associations to enable anaphase I segregation in Drosophila male meiosis. PLoS Genet. 2008;4(10):e1000228. doi: 10.1371/journal.pgen.1000228. PubMed PMID: 18927632; PubMed Central PMCID: PMC2562520.

73. Dion-Cote AM, Barbash DA. Beyond speciation genes: an overview of genome stability in evolution and speciation. Curr Opin Genet Dev. 2017;47:17-23. Epub 2017/08/23. doi: 10.1016/j.gde.2017.07.014. PubMed PMID: 28830007; PubMed Central PMCID: PMCPMC5716907.

74. Romero-Soriano V, Modolo L, Lopez-Maestre H, Mugat B, Pessia E, Chambeyron S, et al. Transposable Element Misregulation Is Linked to the Divergence between Parental piRNA Pathways in Drosophila Hybrids. Genome Biol Evol. 2017;9(6):1450-70. Epub 2017/09/01. doi: 10.1093/gbe/evx091. PubMed PMID: 28854624; PubMed Central PMCID: PMCPMC5499732.

823 75. George P, Jensen S, Pogorelcnik R, Lee J, Xing Y, Brasset E, et al. Increased production
824 of piRNAs from euchromatic clusters and genes in Anopheles gambiae compared with
825 Drosophila melanogaster. Epigenetics Chromatin. 2015;8:50. doi: 10.1186/s13072-015-0041-5.
826 PubMed PMID: 26617674; PubMed Central PMCID: PMC4662822.
827 76. Ferree PM, Barbash DA. Species-specific heterochromatin prevents mitotic chromosome
828 segregation to cause hybrid lethality in Drosophila. PLoS Biol. 2009;7(10):e1000234. Epub
829 2009/10/28. doi: 10.1371/journal.pbio.1000234. PubMed PMID: 19859525; PubMed Central
830 PMCID: PMCPMC2760206.
831 77. Bayes JJ, Malik HS. Altered heterochromatin binding by a hybrid sterility protein in
832 Drosophila sibling species. Science. 2009;326(5959):1538-41. Epub 2009/11/26. doi:
833 10.1126/science.1181756. PubMed PMID: 19933102; PubMed Central PMCID:
834 PMCPMC2987944.
835 78. Henikoff S, Ahmad K, Malik HS. The centromere paradox: Stable inheritance with
836 rapidly evolving DNA. Science. 2001;293(5532):1098-102. doi: DOI 10.1126/science.1062939.
837 PubMed PMID: WOS:000170432600049.
838 79. Malik HS, Henikoff S. Adaptive evolution of cid, a centromere-specific histone in
839 drosophila. Genetics. 2001;157(3):1293-8. PubMed PMID: WOS:000167420000032.
840 80. Rosin L, Mellone BG. Co-evolving CENP-A and CAL1 Domains Mediate Centromeric
841 CENP-A Deposition across Drosophila Species. Developmental Cell. 2016;37(2):136-47. doi:
842 10.1016/j.devcel.2016.03.021. PubMed PMID: WOS:000374712900008.
843 81. Darwin C. On the origin of species by means of natural selection or, The Preservation of
844 favoured races in the struggle for life. London: Electric Book Co.,; 2001.

845 82. Scott JA, Brogdon WG, Collins FH. Identification of single specimens of the Anopheles
846 gambiae complex by the polymerase chain reaction. Am J Trop Med Hyg. 1993;49(4):520-9.
847 Epub 1993/10/01. PubMed PMID: 8214283.
848 83. Fanello C, Santolamazza F, della Torre A. Simultaneous identification of species and
849 molecular forms of the Anopheles gambiae complex by PCR-RFLP. Med Vet Entomol.
850 2002;16(4):461-4. Epub 2003/01/04. PubMed PMID: 12510902.
851 84. Benedict M, Dotson EM. Methods in Anopheles Research:
852 https://www.beiresources.org/Portals/2/VectorResources/2016%20Methods%20in%20Anopheles
853 s%20Research%20full%20manual.pdf; 2015.
854 85. Pitts RJ, Liu C, Zhou X, Malpartida JC, Zwiebel LJ. Odorant receptor-mediated sperm
855 activation in disease vector mosquitoes. Proc Natl Acad Sci U S A. 2014;111(7):2566-71. doi:
856 10.1073/pnas.1322923111. PubMed PMID: 24550284; PubMed Central PMCID: PMC3932880.
857 86. Timoshevskiy VA, Sharma A, Sharakhov IV, Sharakhova MV. Fluorescent in situ
858 Hybridization on Mitotic Chromosomes of Mosquitoes. J Vis Exp. 2012;(67). Epub 2012/09/26.
859 doi: 10.3791/4215. PubMed PMID: 23007640.
860 87. Sharakhova MV, George P, Timoshevskiy V, Sharma A, Peery A, Sharakhov IV.
861 Mosquitoes (Diptera). In: Sharakhov IV, editor. Protocols for Cytogenetic Mapping of Arthropod
862 Genomes. Boca Raton, FL: CRC Press, Taylor & Francis Group; 2015. p. 93-170.

863

864

865 Figure Legends

866 **Fig 1. Morphology and cell content of testes from 2-day-old adult males.** (A) Whole testis,
867 squashed testis, and mature spermatozoa in crushed testis from *An. coluzzii* MOPTI. (B) Normal-

like whole testis, squashed testis, and immature spermatozoa and spermatids in crushed testis from an F1 hybrid of the cross ♀*An. merus* × ♂*An. coluzzii* MOPTI. (C) Underdeveloped whole testis, squashed testis, and undifferentiated cells in crushed testis from an F1 hybrid of the cross ♀*An. coluzzii* MOPTI × ♂*An. merus.* Vertical scale bars – 50 and 20 μm.

Fig 2. Chromosome behavior during meiosis in testes of *An. gambiae.* X chromosomes are labeled with 18S rDNA (red), and Y chromosomes are labeled with retrotransposon *zanzibar* (green). Chromosomes are counterstained with DAPI (blue). Scale bar – 5 μm.

Fig 3. Chromosome behavior during meiosis in testes of interspecies hybrids. (A) ♀*An. merus* × ♂*An. coluzzii* MALI. (B) ♀*An. merus* × ♂*An. coluzzii* MOPTI. (C) ♀*An. merus* × ♂*An. gambiae* ZANU. X chromosomes are labeled with 18S rDNA (red), and Y chromosomes are labeled with retrotransposon *zanzibar* (green). Chromosomes are counterstained with DAPI (blue). Scale bar – 5 μm.

Fig 4. Chromosomal and molecular abnormalities in interspecies hybrids. (A) Left panel: Lengths of metaphase chromosomes in *An. gambiae* ZANU males (filled boxplots) and in F1 hybrid males from the cross ♀*An. merus* × ♂*An. gambiae* ZANU (open boxplots). Right panel: Ratios of the lengths of chromosomes between F1 hybrids and *An. gambiae* ZANU. X and Y – sex chromosomes. 2 and 3 – autosomes. Statistical significance was assessed with a two-sample pooled *t*-test. (B) Confocal images of primary spermatocytes with FISH to demonstrate pairing and unpairing of X (red) and Y (green) chromosomes in *An. coluzzii* MOPTI males and F1 hybrid males from the ♀*An. merus* × ♂*An. coluzzii* MOPTI cross. (C) Percentage of the X and Y

chromosome pairing in primary spermatocytes of six *An. coluzzii* MOPTI males and six F1 hybrid males from the ♀*An. merus* × ♂*An. coluzzii* MOPTI cross. Statistical significance was assessed with a two-sample pooled *t*-test. (D) Expression of meiotic (*Ams, mts, Dzip1l, β2-tubulin*) and pre-meiotic (*vasa*) germline-specific genes in testes of *An. coluzzii*, F1 hybrids of ♀*An. merus* × ♂*An. coluzzii* MOPTI (F1M×C), and F1 hybrids of ♀*An. coluzzii* MOPTI × ♂*An. merus* (F1C×M) analyzed by RT-PCR. *AgS7* – an endogenous control gene. R – reproductive tissues, B – rest of mosquito body.

Fig 5. Genomic rearrangements of meiotic chromosomes in testes of interspecies hybrids. (A) A translocation of the fragment of the *An. merus* X chromosome to the *An. coluzzii* autosome 2 in a hybrid from the ♀*An. merus* × ♂*An. coluzzii* MALI cross. The red arrow points to the translocated X-chromosome ribosomal locus labelled by 18S rDNA (red). (B) A duplication of the segment involving the rDNA locus within the *An. merus* X chromosome in a hybrid from the cross ♀*An. merus* × ♂*An. gambiae* ZANU. The red arrow indicates the new positions of the segment with the ribosomal locus labelled by 18S rDNA (red). Chromosomes are counterstained with DAPI.

Fig 6. Schematic representation of testis development in pure species and reciprocal F1 hybrids of the *An. gambiae* complex.

Fig 7. Scheme of male meiosis in pure species and interspecies hybrids of the *An. gambiae* complex. Unlike pure species, X and Y chromosomes in meiotic prophase I of hybrids are

913 largely unpaired. Instead of a reductional division, primary spermatocytes in interspecies hybrids
914 undergo an equational mitotic division leading to diploid nonmotile sperms.
915

916 ## Supporting Information

917 **S1 Fig. Chromosome behavior during meiosis in testes of *An. coluzzii* MOPTI.** X
918 chromosomes are labeled with 18S rDNA (red), and Y chromosomes are labeled with
919 retrotransposon *zanzibar* (green). Chromosomes are counterstained with DAPI (blue). Scale bar
920 – 5 μm.
921

922 **S2 Fig. Chromosome behavior during meiosis in testes of *An. merus* MAF.** Sex
923 chromosomes are labeled with 18S rDNA (red) and satellite AgY53B (green). Chromosomes are
924 counterstained with DAPI (blue). Scale bar – 5 μm.
925

926 **S3 Fig. Sizes and sex chromosome content of spermatids in pure species and interspecies**
927 **hybrids.** (A) Spermatids from a 2-day-old adult of *An. coluzzii* MOPTI. (B) Spermatids from a
928 5-day-old adult F1 hybrid from the cross ♀*An. merus* × ♂*An. coluzzii* MOPTI. The X and Y
929 chromosomes are visualized with 18S rDNA (red) and retrotransposon *zanzibar* (green),
930 respectively. Chromatin is counterstained with DAPI (blue). The insets show magnified images
931 of spermatids.
932

933 **S4 Fig. Visualization of sex chromosomes in a degenerate testis of a hybrid adult from the**
934 **cross ♀*An. coluzzii* MOPTI × ♂*An. merus*.** (A) DAPI-stained male accessory glands and an
935 underdeveloped testis of a one-day-old hybrid adult. (B) Whole-mount FISH of the degenerate

testis with 18S rDNA (red) and satellite AgY53B (green) detects the interphase X and Y chromosomes, respectively. Chromatin is counterstained with DAPI (blue).

S5 Fig. Increased lengths of chromosomes in testes of interspecies F1 hybrids. Left panel: Lengths of metaphase chromosomes in *An. coluzzii* MOPTI (filled boxplots) and in F1 hybrid males from the cross *An. merus* × ♂*An. coluzzii* MOPTI (open boxplots). Right panel: Ratios of the lengths of chromosomes between hybrids and pure species. X and Y – sex chromosomes. 2 and 3 – autosomes. Statistical significance was assessed with a two-sample pooled *t*-test.

S6 Fig. Delays in the X chromosome segregation during anaphase in primary spermatocytes of F1 hybrid males from the cross *An. merus* × ♂*An. gambiae* ZANU.

S7 Fig. Visualization of sex chromosomes in testes of a pure species and interspecies F1 hybrid. (A, B) Testis of a one-day-old adult of *An. coluzzii* MOPTI. (C, D) Testis of a one-day-old adult F1 hybrid of the cross ♀*An. merus* × ♂*An. coluzzii* MOPTI. Whole-mount FISH with 18S rDNA (red) and satellite AgY53B (green) is performed to detect the X and Y chromosomes, respectively. Chromatin is counterstained with DAPI (blue).

S1 Table. Sizes of metaphase chromosomes in pure species and interspecies F1 hybrids of the *An. gambiae* complex.

S2 Table. Numbers and percentages of primary spermatocytes with paired and unpaired sex chromosomes.

959

960 **S1 Movie. Sperm motility in a crushed testis from a 2-day-old adult of *An. merus.***

961

962 **S2 Movie. Sperm motility in a crushed normal-like testis from a 2-day-old adult hybrid of**

963 **the cross ♀*An. merus* × ♂*An. coluzzii* MOPTI.**

964

965

966

967

968

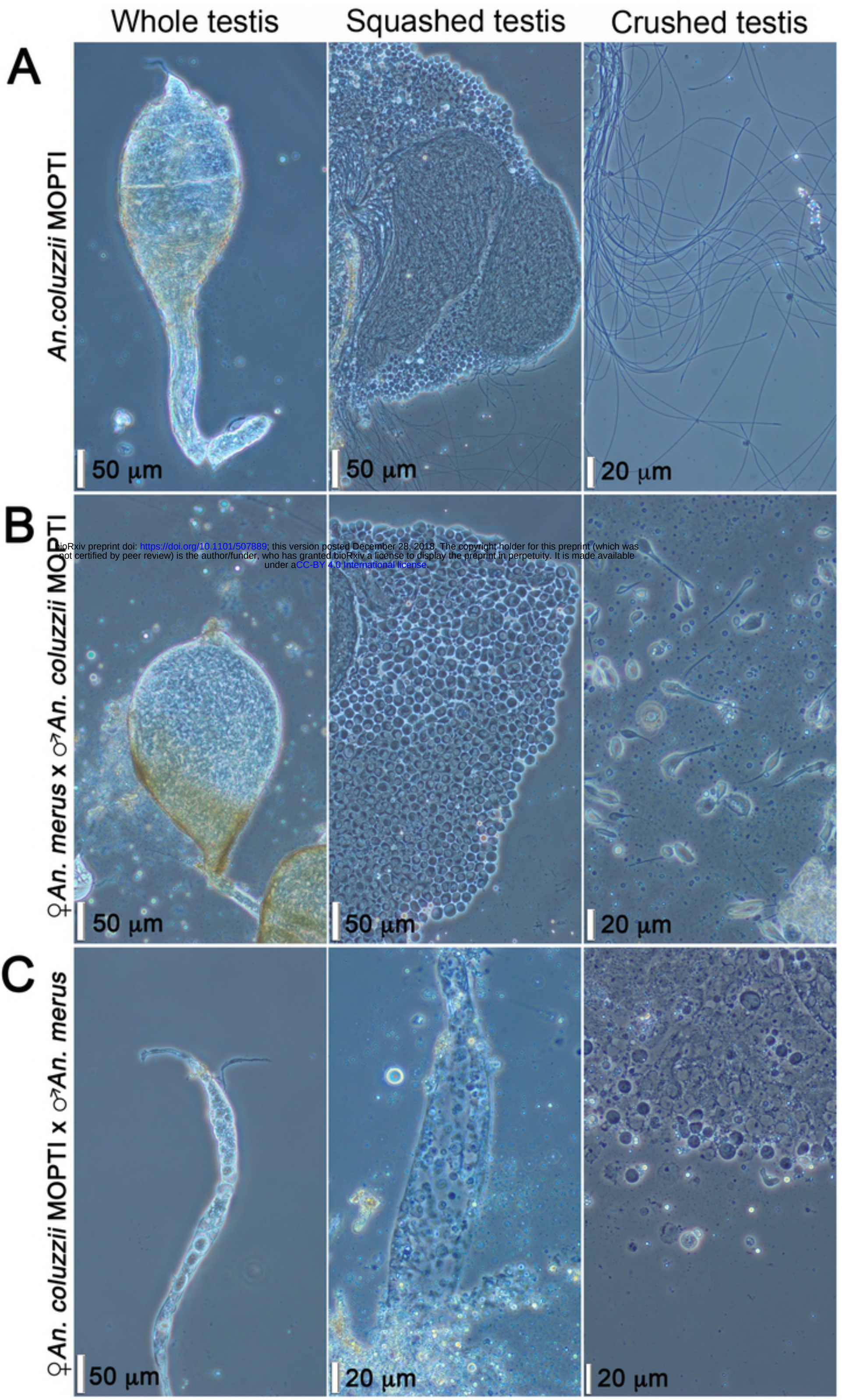

Figure 1

Figure 2

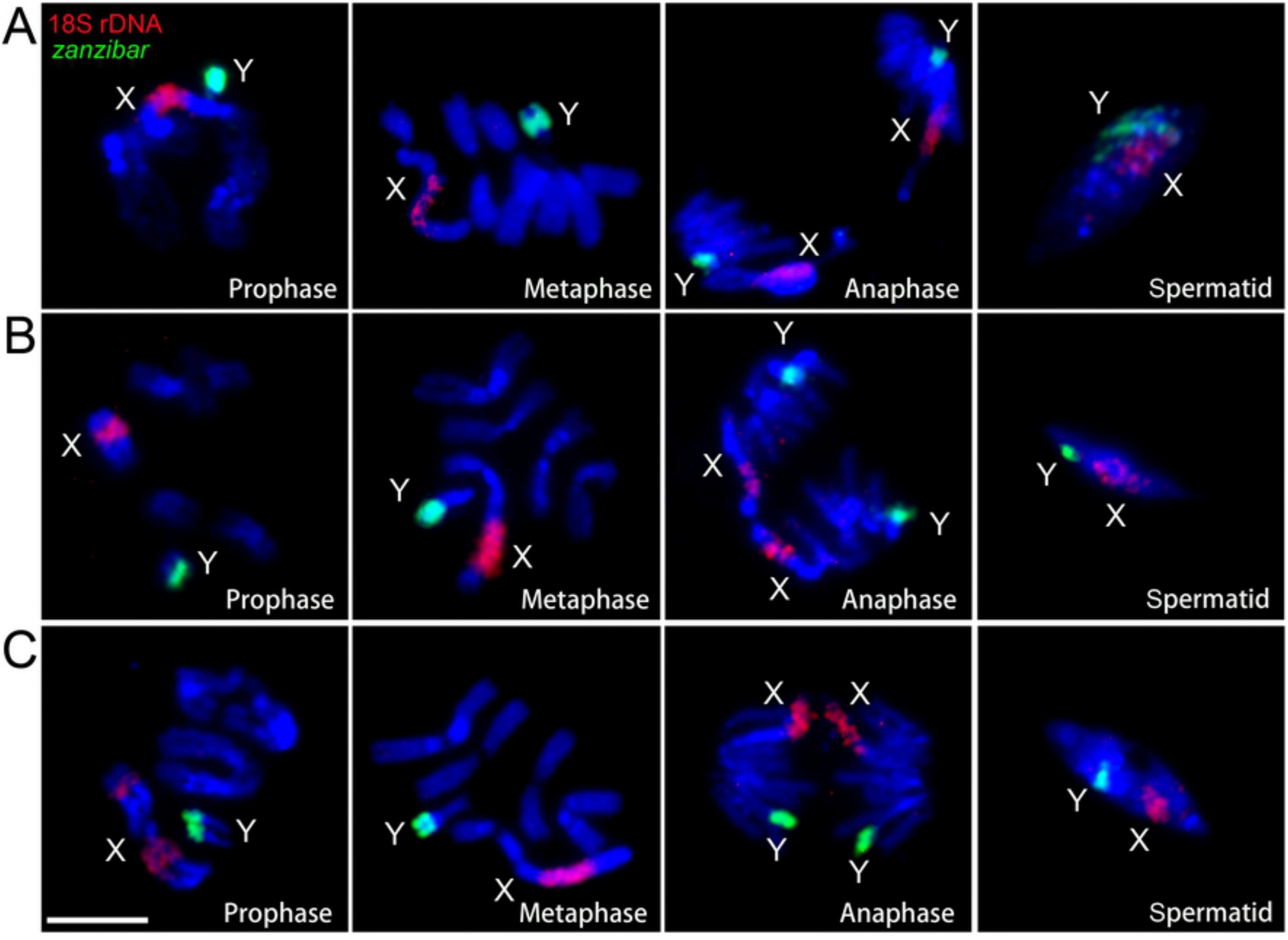
A
18S rDNA
zanzibar
X
Y
Prophase
Metaphase
Anaphase
Spermatid
B
C

Figure 3

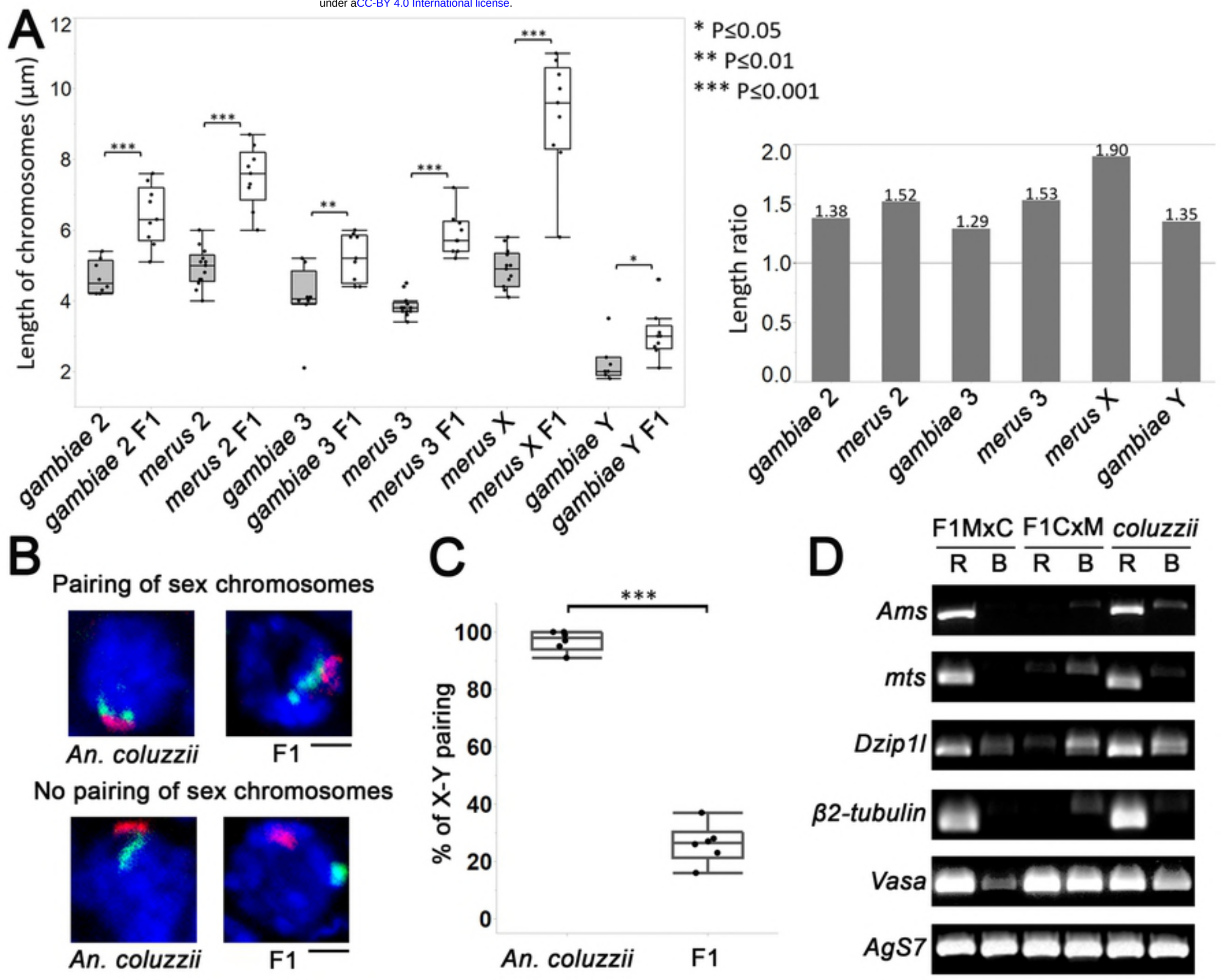

Figure 4

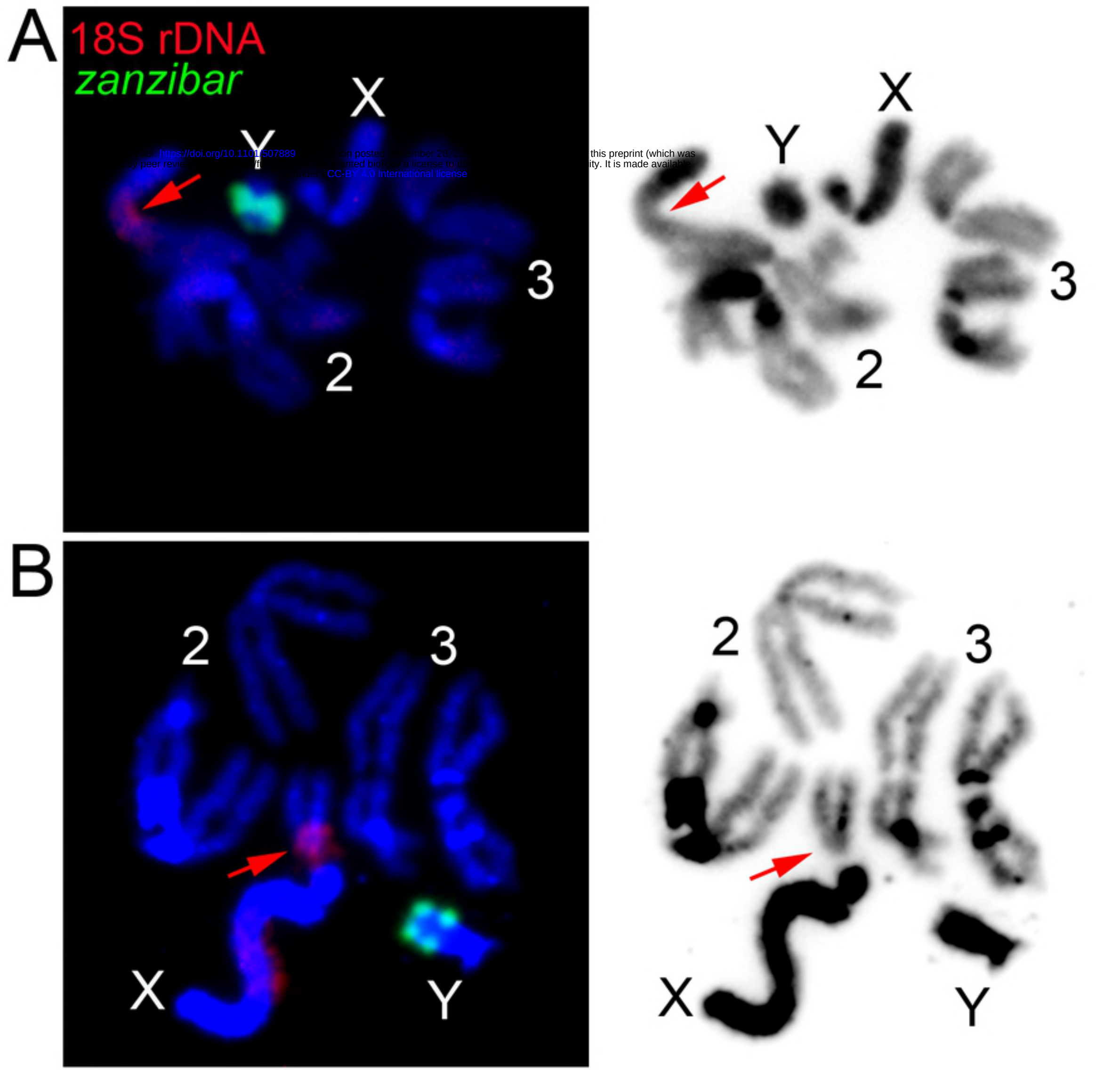

Figure 5

Testis of F1 ♀ *An. coluzzii* × ♂ *An. coluzzii*

Stem cell divisions

Gonial cell amplificaiton

Growth and gene expression

Meiotic divisions

Spermatid differentiation

Mature haploid spermatozoa

Testis of F1 ♀ *An. merus* × ♂ *An. coluzzii*

Stem cell divisions

Gonial cell amplificaiton

Growth and gene expression

Meiotic prophase I is followed by mitotic anaphase

Delayed spermatid differentiation and partially developed diploid spermatozoa

Testis of F1 ♀ *An. coluzzii* × ♂ *An. merus*

Arrested spermatogenesis with undifferentiated cells

Hub

Gonial cells

Premeiotic cells

Spermatids

Cyst cells

Meiotic prophase I with X-Y chromosome pairing

Meiotic prophase I with no X-Y chromosome pairing

Anaphase I with homologous chromosome segregations

Abnormal anaphase with both X and Y sister chromatid segregations in hybrids

Anaphase II with sister chromatid segregations

Diploid spermatozoa

Haploid spermatozoa

Figure 6

Normal male meiosis in pure species

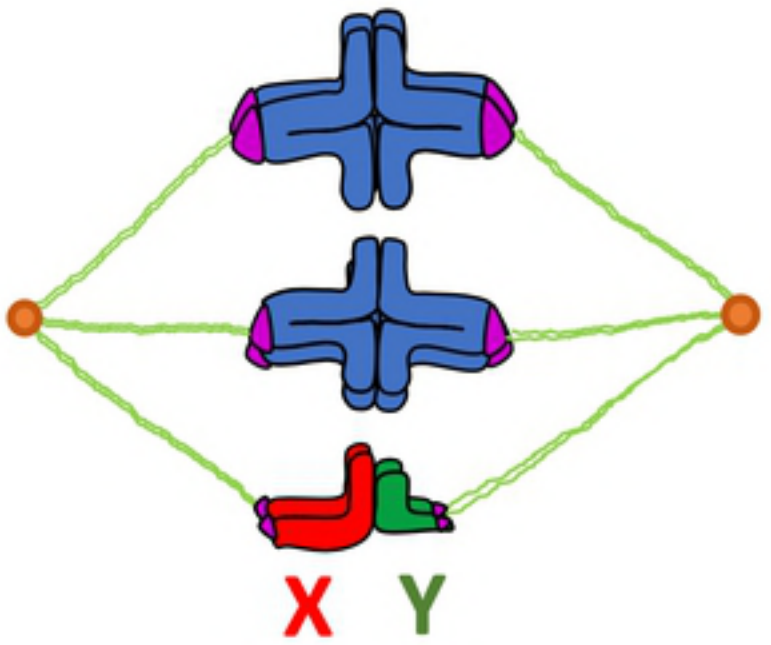

Prophase I

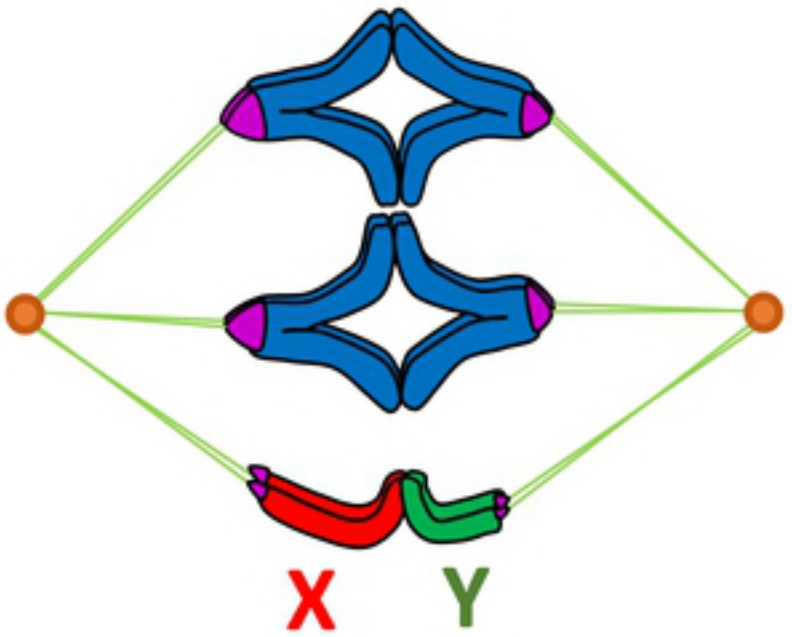

Anaphase I

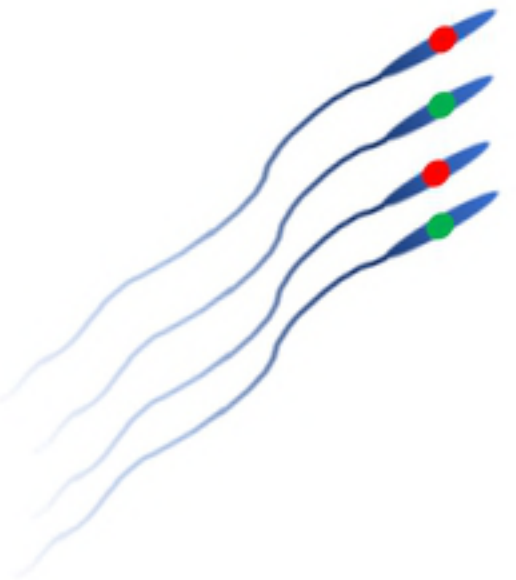

Normal sperm

Failed male meiosis in F1 hybrids

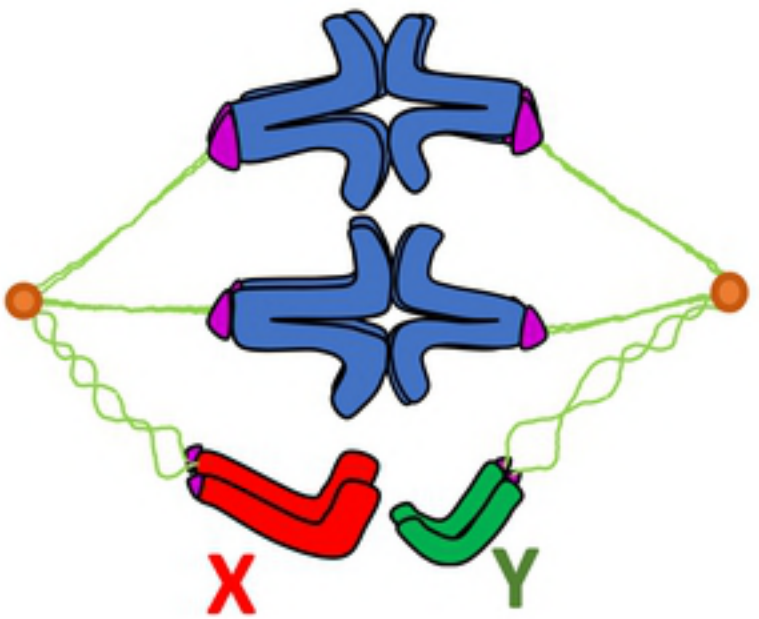

Prophase I

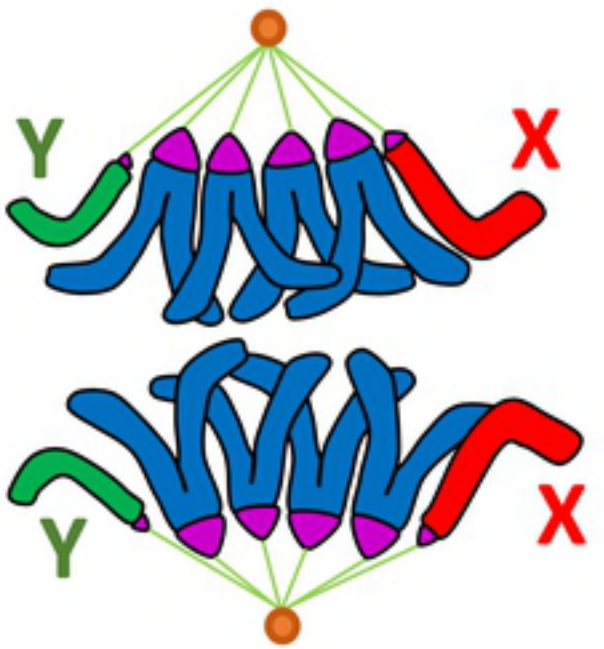

Anaphase

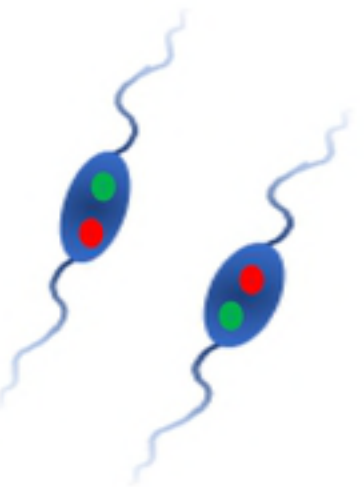

Diploid sperm

Figure 7